Coordination Chemistry Reviews 254 (2010) 1358–1382

Contents lists available at ScienceDirect

Coordination Chemistry Reviews

journal homepage: www.elsevier.com/locate/ccr

Review

o-Dithiolene and *o*-aminothiolate chemistry of iron: Synthesis, structure and reactivity

Stephen Sproules*, Karl Wieghardt

Max-Planck-Institut für Bioanorganische Chemie, Stiftstrasse 34-36, D-45470 Mülheim an der Ruhr, Germany

Contents

ARTICLE INFO

Article history:
Received 22 September 2009
Accepted 6 December 2009
Available online 18 January 2010

Keywords:
Iron
Dithiolene
Aminothiolate
Ligand radical
Spectroscopy
Reactivity
Electronic structure

ABSTRACT

Homoleptic complexes with an iron center bound by two *o*-dithiolene or *o*-aminothiolate ligands, or one tetradentate aminothiolate ligand will be discussed in the context of their molecular and electronic structures. These compounds are predominantly dimeric and exhibit rich redox chemistry due to the multiple redox active iron and ligand components. Their reaction with small molecules, namely, pyridines, amines, phosphines, phosphites, arsines, stibines, cyanide, halogens, and nitric oxide, has produced extensive libraries of compounds that are also reviewed. These five- and six-coordinate mononuclear and dinuclear adduct complexes access an incredibly broad range of iron and ligand spin and oxidation states that generates a multitude of electronic structures.

Abbreviations: S_{Fe}, spin state of iron ion; S_L, spin state of ligand(s); S_t, total spin ground state; μ_{eff}, effective magnetic moment; ZFS, D, zero-field splitting; E/D, rhombicity; *J*, coupling constant; *g*, *g*-value; *A*, magnetic hyperfine; δ, isomer shift; ΔE_Q, quadrupole splitting; DFT, density functional theory; MO, molecular orbital; DOMO, doubly occupied molecular orbital; SOMO, singly occupied molecular orbital; HOMO, highest occupied molecular orbital; LUMO, lowest unoccupied molecular orbital; S, orbital integral overlap; LMCT, ligand-to-metal charge transfer; LLCT, ligand-to-ligand charge transfer; LLIVCT, ligand-to-ligand intervalence charge transfer; UV, ultraviolet; Vis, visible; EPR, electron paramagnetic resonance; py, pyridine; ^{t}Bu-py, 4-*tert*-butylpyridine; dmf, *N*,*N*′-dimethylformamide; dmso, dimethylsulfoxide; thf, tetrahydrofuran; dppe, diphenylphoshinoethane; dppet, diphenylphosphinoethylene; dppm, diphenylphoshinomethane; dppb, diphenylphoshinobenzene; dppa, diphenylphoshinoacetylene; *i*-quin, isoquinoline; pic, picoline; rad$^{\bullet+}$, 2-(*p*-*N*-methylpyridinium)-4,4,5,5-tetramethylimidazoline-1-oxyl; idzm$^{\bullet+}$, 2-(*p*-pyridyl)-4,4,5,5-tetramethylimidazolinium; G, Gauss.

* Corresponding author.

0010-8545/$ – see front matter © 2009 Elsevier B.V. All rights reserved.
doi:10.1016/j.ccr.2009.12.012

1. Introduction

The term "dithiolene" was introduced as a simple nomenclature to describe bidentate sulfur-donor ligands connected via an unsaturated carbon–carbon bond [1,2]. It is used to encompass all forms of the ligand without giving bias to one particular structure or valence formalism [3,4]. The description was required, as experimental evidence accumulated over the last 50 years would testify, that this ligand is highly redox noninnocent; the redox levels are presented in Scheme 1. In the 1960s, procedures for the synthesis and isolation of dithiolene ligands were developed that spurred an enormous upsurge in the isolation and characterization of then novel coordination compounds [3]. These complexes possessed rich redox chemistry and intriguing electronic structures that surfaced when redox active ligand(s) were tethered to a transition metal; iron complexes were among the first to be prepared and characterized [5].

It was some years later that the chemistry of analogous dioxolene ligands (chiefly catechols) was developed [7]. It is quite interesting to observe that although dithiolene and dioxolene ligands have the same three redox levels (dianionic, radical monoanion, neutral) there appears to be an unambiguous acceptance of the existence of *O,O′*-semiquinonate(1-) π radicals in coordination compounds while the coordination of *S,S′*-dithiosemiquinonate(1-) π radical ligands have been largely ignored or even explicitly ruled out [8,9]. The coordination chemist's primary method for determining ligand radical character has been (and still is) X-ray crystallography, and an open-shell semiquinone ligand is easily discriminated from the closed-shell neutral quinone and dianionic catecholate forms by significant differences in the C–O bond distances and aptly named quinoidal distortion of the six-membered ring that is generally beyond the estimated standard deviations, 3σ (Fig. 1) [10].

Although sulfur is less electronegative than oxygen, considerably more spin density resides on the sulfur atom (75% cf. 45% for oxygen, Fig. 1) [11], and therefore less spin density is delocalized over the phenyl ring. As such, the variation in the C–S and C–C bond lengths is typically inside the 3σ level, hampering an assignment of the redox level of the ligand by X-ray crystallography. However, it is quite interesting albeit expected, that dithiosemiquinone ligands do exist in coordination compounds, and we have demonstrated that the correct electronic structures are revealed using the combination of high-quality X-ray crystallography, spectroscopy, and theoretical calculations [11–15].

The history of aminothiolate [16] ligands closely parallels that of dithiolates, since they share many similarities [17]. These ligands carry an additional dimension in that the nitrogen ligand can be doubly or singly protonated, as well as alkylated [16], which increases its versatility over dithiolenes; the redox levels of aminothiolates are shown in Scheme 2. As such, there are several examples of aminothiolate moieties in polydentate ligands coordinating iron that possess novel molecular structures and reactivities that will not be included in this article [18]. The advantage of N,S coordination about iron was realized when it became apparent that it resembled numerous biological systems, in particular the nitrogenases [19]. Thus, these complexes served as both structural and functional models through adopting uncommon structures,

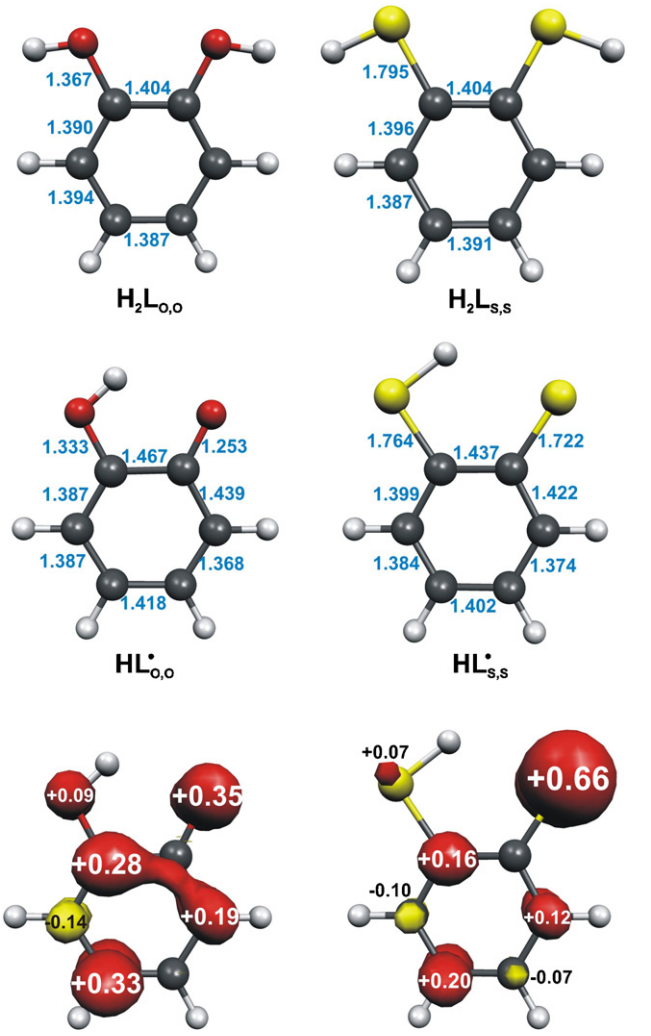

Fig. 1. Calculated molecular structures of uncoordinated catechol ($H_2L_{O,O}$) and benezene-1,2-dithiol ($H_2L_{S,S}$) and their deprotonated one-electron oxidized benzosemiquinone ($HL^{\bullet}_{O,O}$) and dithiobenzosemiquinone ($HL^{\bullet}_{S,S}$) radical forms. Below are the Mulliken spin density plots for the $S = 1/2$ neutral radicals ($HL^{\bullet}_{O,O}$, left) and ($HL^{\bullet}_{S,S}$, right) [11]. Red: α-spin density; β-spin density. Red spheres represent oxygen atoms; yellow spheres: sulfur; black spheres: carbon; white spheres: hydrogen atoms.

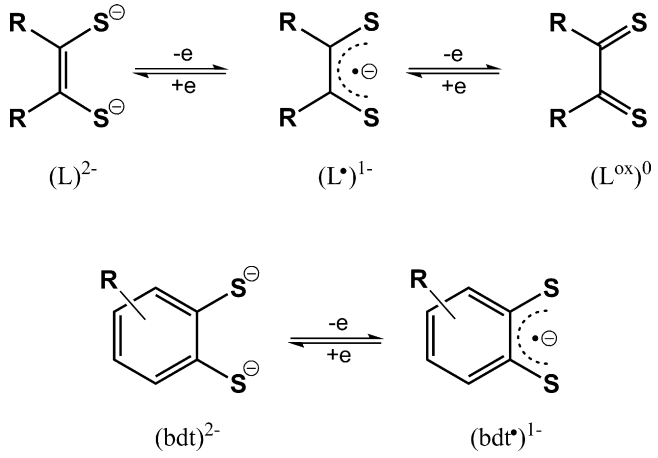

Scheme 1. Olefinic (top) and aromatic (bottom) dithiolene ligand redox levels [6].

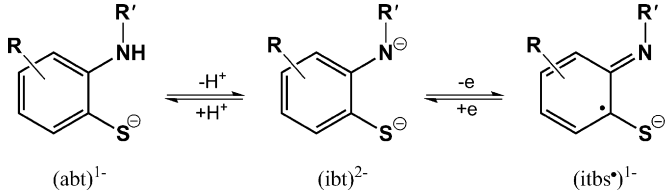

Scheme 2. Redox and protonation levels for aminobenzenethiolate ligands [16].

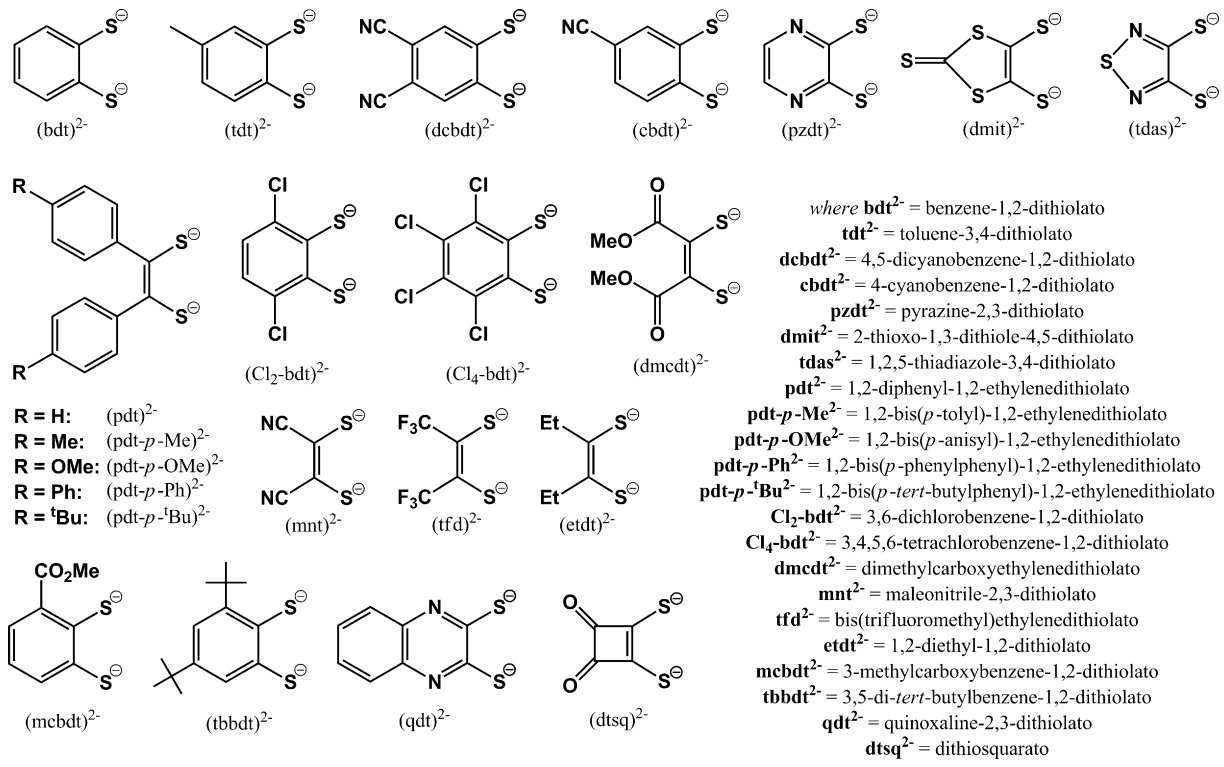

Scheme 3. Dithiolene ligands and their abbreviations.

stabilizing unusual metal oxidation states, and creating vacant coordination sites and electron deficiency [20].

Sellmann et al. published three papers exclaiming that high-valent Fe(IV) and Fe(V) ions were stabilized by dithiolene and aminothiolate ligands implying their redox innocence [9,21,22]. The iron ions in the compounds in question, $[Fe(bdt)_2(PMe_3)_2]$ [9], $[Fe(bdt)_2(PMe_3)]$ [9], $[Fe(bmae)_2(P^nPr_3)]$ [22], $[Fe(bmae)_2I]$ [21], where bdt = benzene-1,2-dithiolate (Scheme 3) and bmae = 1,2-bis(mercaptoanilino)ethane (Scheme 4) [23], have a formal oxidation state [24] of +IV, +IV, +IV, and +V, respectively. However, the observation of intense electronic transitions in the near-infrared (>600 nm) region is strong evidence for the presence of oxidized ligands, and showed that oxidation state assignment based on X-ray crystallography was ambiguous at best, particularly for structures solved at room temperature. So, despite their long history in coordination chemistry, Fe-dithiolene and Fe-aminothiolate complexes have only very recently received the kind of spectroscopic and theoretical examination necessary to correctly assign their true electronic structure [25–27]. For example, a reevaluation of the aforementioned high-valent Fe complexes showed that indeed the ligands were oxidized rather than the metal [14].

In this article we will present an overview of bis(dithiolene) and bis(aminothiolate) iron complexes, as well as tetradentate N_2S_2 complexes of iron, with an emphasis on their molecular and electronic structure that affords a physical oxidation state [24] assignment of both the redox active ligand and metal. A list of the ligands and their abbreviations is presented in Schemes 3 and 4. Furthermore, we will provide an overview of reactions of these homoleptic complexes with various small molecules, such as Lewis bases that typically lead to five- or six-coordinate adduct complexes with quite varied electronic structures that cover a range of ligand oxidation states, and iron oxidation and spin states.

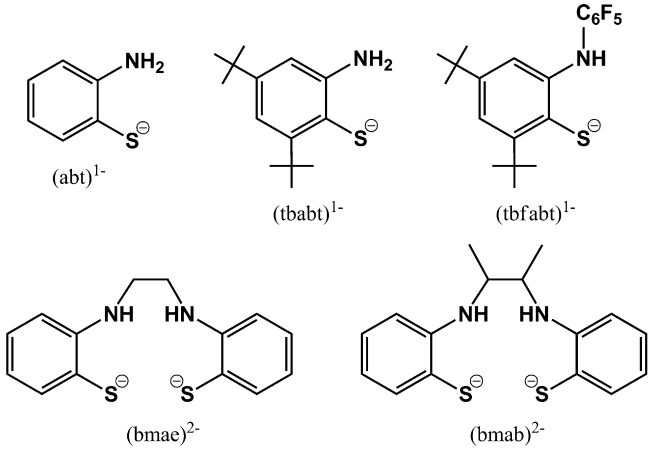

where **abt**$^{1-}$ = 2-aminobenzenethiolato
tbabt^{1-} = 4,6-di-*tert*-butyl-2-aminobenzenethiolato
tbfabt^{1-} = 4,6-di-*tert*-butyl-2-[(pentafluorophenyl)amino]benezenethiolato
bmae^{2-} = 1,2-bis(mercaptoanilino)ethane
bmab^{2-} = 1,2-bis(mercaptoanilino)butane

Scheme 4. Aminothiolate ligands and their abbreviations [16].

2. Mononuclear complexes

2.1. Bis(dithiolene)

Mononuclear Fe bis(dithiolene) complexes are extremely rare, with just four crystallographically characterized examples. The first ever reported crystal structure was $[PPh_4]_2[Fe^{II}(S_2C_4O_2)_2]$ [28], which contains the quite unusual dithiosquarato ligand $(S_2C_4O_2)^{2-}$ (Fig. 2). This complex, along with $[Fe^{II}(SPh)_4]^{2-}$ were prepared to model the $Fe^{II}S_4$ site in rubredoxins and horse liver alcohol

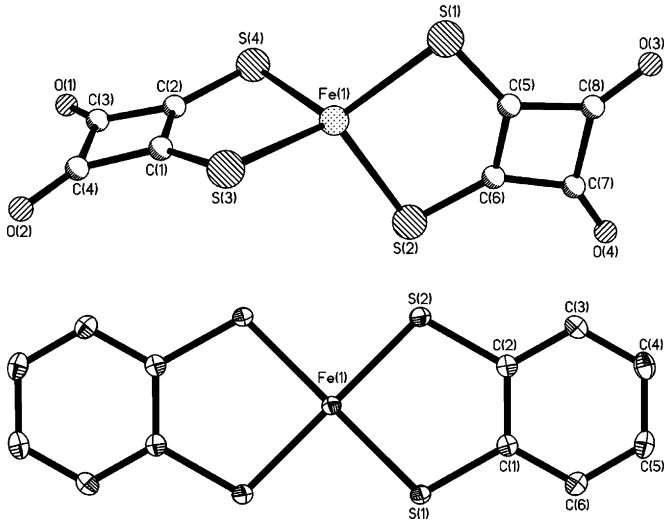

Fig. 2. Crystal structures of $[Fe(dtsq)_2]^{2-}$ [28], and $[Fe(bdt)_2]^{2-}$ [30].

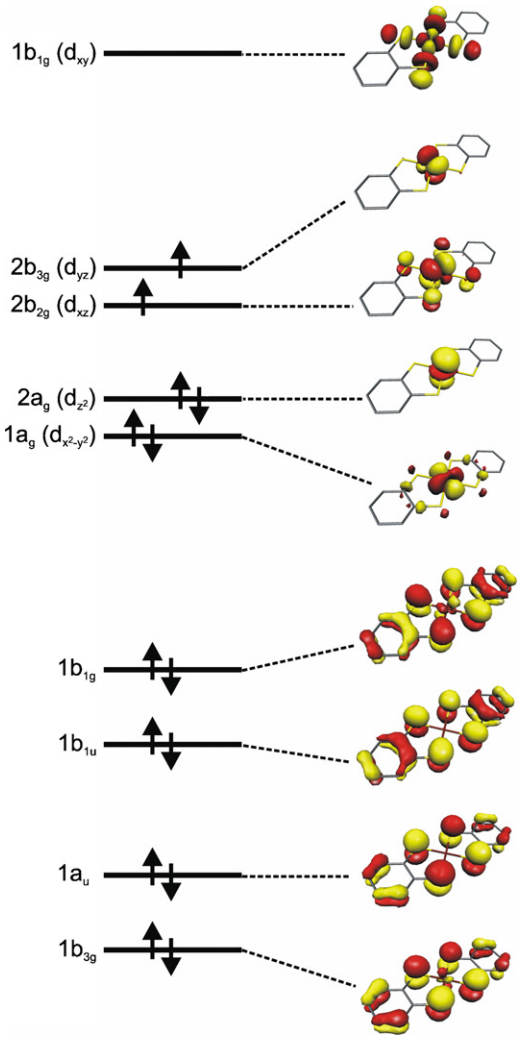

Fig. 3. Qualitative MO scheme for $[Fe^{II}(bdt)_2]^{2-}$ ($S=1$). The $1b_{1u} \rightarrow 2b_{2g}$ transition is clearly ligand-to-metal charge transfer and has very little intensity due to the poor donor–acceptor orbital overlap. The large ZFS arises from spin-conserving $d_{x^2-y^2}$ and d_{z^2} to d_{xz} and d_{yz} ligand field transitions, with smaller contributions from SOMO–SOMO (d_{xz} and d_{yz}) spin flip transitions [30].

dehydrogenase. Interestingly, though the sulfur-donor ligands are bidentate, this ferrous complex possesses near-perfect tetrahedral geometry; the dihedral angle between the FeS_2 planes is 85.8°. The Fe–S bond lengths of 2.389 Å are longer than those of $[Fe^{II}(SPh)_4]^{2-}$ because the bond is more ionic. The constraints imposed by the cyclobutenone moiety produce a large S–Fe–S angle of 95.7° and a S···S distance of 3.541 Å. The large dithiolate bite angles result from contributions from two resonance structures that produce very short C–S bond lengths of 1.688 Å [29]. This creates a very poor donor ligand and the observed tetrahedral geometry. As expected, the central ion is high-spin Fe(II) ($S_{Fe}=2$); the room temperature effective magnetic moment (μ_{eff}) is 5.0 μ_B consistent with four unpaired electrons. The low-temperature region (<50 K) was modeled using a zero-field splitting (ZFS) parameter $D=+9.2\ cm^{-1}$ and rhombicity $E/D=0.27$. Applied-field Mössbauer spectroscopy recorded a very large isomer shift, $\delta=0.668\ mm\ s^{-1}$ and quadrupole splitting, $\Delta E_Q=-3.97\ mm\ s^{-1}$ at 80 K (Table 2), typical of high-spin Fe(II).

In 1984, Sellmann et al. produced $[AsPh_4]_2[Fe(bdt)_2]$ from the combination of $FeCl_2{\cdot}4H_2O$ and Li_2bdt under an anaerobic atmosphere (Fig. 2) [31]. The lithium salt of the dithiolene ligand was prepared from the reaction of benzene-1,2-dithiol ($bdtH_2$) and *n*-butyllithium in hexane. The crystal structure of this salt identified well separated cations and anions in a 2:1 ratio. The $[Fe(bdt)_2]^{2-}$ anion is perfectly square planar, in stark contrast to the bis(dithiosquarato) complex described above. At this time, a room temperature magnetic moment of 3.55 μ_B was reported, suggesting an $S_t=1$ state, and later, the zero-field Mössbauer data were collected for $[NMe_4]_2[Fe(bdt)_2]$ [32], with $\delta=0.435\ mm\ s^{-1}$ and $\Delta E_Q=1.161\ mm\ s^{-1}$ at 80 K (Table 2). A methoxy-ester-substituted benzenedithiolate ligand, 2-methylcarboxybenzene-1,2-dithiolate $(mcbdt)^{2-}$ was prepared by Sellmann et al. in an attempt to isolate water soluble complexes [33]. The planar $[AsPh_4]_2[Fe(mcbdt)_2]$ complex synthesized under anaerobic conditions was structurally characterized; its metric parameters mirror those of $[AsPh_4]_2[Fe(bdt)_2]$. Only one stereoisomer was found to be present in solution: the *trans* isomer, thus the iron sits on the crystallographic inversion center. It also afforded an effective magnetic moment of 2.96 μ_B at room temperature. The structure of $[Fe(bdt)_2]^{2-}$ ion, isolated as the $[HNEt_3]^+$ salt [30], was repeated some years later with near-identical metrical parameters. The data were collected at 100 K, which greatly reduced the estimated standard deviation, and gave an average C–S bond length of 1.769 Å and six equidistant C–C bonds (average 1.398 Å) in the aromatic ring, clearly indicated two closed-shell dithiolate dianion ligands bound to a ferrous ion.

A thorough spectroscopic and theoretical examination of $[Fe(bdt)_2]^{2-}$ elucidated its electronic structure [30]. Variable-field, variable-temperature magnetic susceptibility measurements gave $\mu_{eff}=3.18\pm0.01\ \mu_B$ in the temperature range of 50–300 K. Below 50 K, the data was modeled with $D=+28\ cm^{-1}$ and $E/D=0.08$. Therefore, the central ion is intermediate-spin Fe(II), $S_{Fe}=1$. Applied-field measurements could only be accounted for using the large positive value for D, thus confirming the triplet ground state. A $^3B_{1g}$ ground state was computed for this dianion, whose electronic configuration is $(1a_g)^2(2a_g)^2(1b_{3g})^2(1a_u)^2(1b_{2g})^2(1b_u)^2(2b_{2g})^1(2b_{3g})^1(1b_{1g})^0$. The molecular orbital (MO) manifold is shown in Fig. 3 and Mulliken spin density plot in Fig. 4. Here, the intermediate-spin ferrous ion is seen as $(d_{x^2-y^2})^2(d_{z^2})^2(d_{xz})^1(d_{yz})^1(d_{xy})^0$, with two unpaired α-spin electrons localized on the metal. The large ZFS for this Fe(II) ion stems from spin-conserving d–d transitions from the doubly occupied $d_{x^2-y^2}$ and d_{z^2} orbitals (DOMOs) to the singly occupied d_{xz} and d_{yz} orbitals (SOMOs) (Fig. 3). The DFT-derived $D=+18\ cm^{-1}$ agrees nicely with the experiment both in magnitude and sign.

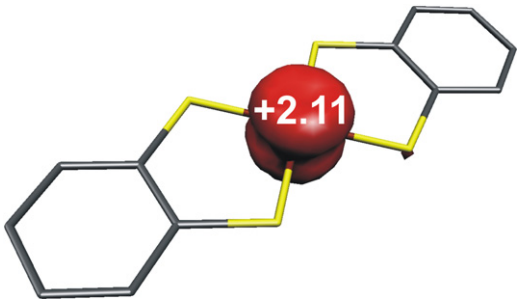

Fig. 4. Mulliken spin density plot for $[Fe^{II}(bdt)_2]^{2-}$ (red: α-spin; yellow: β-spin).

An interesting comparison was made with the isoelectronic $[Co(bdt)_2]^{1-}$ [30], which is deep blue in color compared to the yellow iron compound. Both have similar ZFS values and the same ground state electronic configuration. The prominent difference in color, noticeable in the electronic absorption spectra, is due to the 50% Co composition of the $2b_{2g}$ SOMO, whereas this MO has >90% Fe character in $[Fe(bdt)_2]^{2-}$. The larger effective nuclear charge of Co stabilizes the 3d orbitals such that they are at a comparable energy to the S 3p orbitals of the dithiolene ligands. This generates highly covalent frontier orbitals that render assignment of physical oxidation states for the ligand and metal impossible. As such, it is best represented by the resonance forms $[Co^{III}(bdt^{2-})(bdt^{2-})]^{1-} \leftrightarrow [Co^{II}(bdt^{2-})(bdt^{\bullet 1-})]^{1-} \leftrightarrow [Co^{II}(bdt^{\bullet 1-})(bdt^{2-})]^{1-}$. The existence of partial ligand radicals gives rise to an intense absorption band ($1b_{1u} \rightarrow 2b_{1g}$) in the visible region with both ligand-to-metal (LMCT) and ligand-to-ligand charge transfer (LLCT) character from which the deep blue color is derived. In contrast, the low effective nuclear charge of the intermediate-spin Fe(II) ion provides a large energy separation between the Fe 3d orbitals and the S 3p orbitals such that the SOMOs ($2b_{2g}$ and $2b_{3g}$) are clearly metal-based (Fig. 3). Therefore, the equivalent $1b_{1u} \rightarrow 2b_{2g}$ electronic transition occurs in the UV region of the spectrum and has very little intensity resulting in a yellow compound.

Air-sensitive $[Fe(L)_2]^{2-}$ (L = dithiolene) rapidly oxidizes in air to give a $[Fe^{III}(L)_2]^{1-}$ complex that, in all but three examples [34–36], dimerizes through formation of Fe–S bonds [37]. The most prominent exception to this process was reported by Almeida et al. with the crystallographic characterization of $[NBu_4][Fe^{III}(qdt)_2]$ [35], containing the planar aromatic dithiolate ligand, quinoxaline-2,3-dithiolate $(qdt)^{2-}$. The C–S and C_{arom}–C_{arom} bond distances of 1.737 and 1.475 Å suggest some degree of ligand oxidation, however, the highly electron withdrawing pyrazine ring leads to similar intraligand bond distances in other complexes with this ligand [38], such that this complex is formulated as a central Fe(III) ion bound by two closed-shell dithiolate ligands. With no steric encumbrance supplied by the dithiolene ligand, the square planar monomeric structure is stabilized by short contacts between the Fe ion and the $[NBu_4]^+$ countercations. There are additional interactions between the $(qdt)^{2-}$ ligands of adjacent monoanions. The original magnetic susceptibility measurement showed temperature-independent magnetic moment of 2.34 μ_B which was erroneously described as a low-spin ferric ion ($S_{Fe} = 1/2$) with $g = 2.7$! Following the same synthetic procedure but using $[AsPh_4]^+$ countercations leads to the standard dimeric structure $[AsPh_4]_2[Fe^{III}{}_2(qdt)_4]$ [35]; so the countercation tilts the balance between monomeric and dimeric entities. A re-investigation of this complex produced a magnetic moment of 4.2 μ_B [39], with the low-temperature region below 50 K modeled using $D = +16.2\ cm^{-1}$. Recrystallization of this mononuclear species leads to a dimeric complex, as characterized by its Mössbauer parameters and magnetic moment, highlighting the delicate equilibrium between monomer and dimer in solution. These parameters are consistent with an intermediate-spin ferric $S_{Fe} = 3/2$ ion. The Mössbauer spectrum afforded a single quadrupole doublet with an isomer shift $\delta = 0.37\ mm\ s^{-1}$ and quadrupole splitting $\Delta E_Q = 3.02\ mm\ s^{-1}$ at 80 K (Table 2). Such a large quadrupole splitting, as will be discussed for the dimeric complexes, is incompatible with a low-spin ferric ion. It is also worthy to note the decrease in the isomer shift and dramatic increase in the quadrupole splitting when oxidizing $[Fe^{II}(L)_2]^{2-}$ to $[Fe^{III}(L)_2]^{1-}$, consistent with a metal-centered process. The calculated Mössbauer parameters are in good agreement with a $S_t = 3/2$ ground state, which is in keeping with simple ligand field theory for four-coordinate, square planar d^5 complexes.

The second example surfaced very recently in attempts to prepare diffraction-quality crystals $[CoCp_2]_2[Fe_2(pdt\text{-}p\text{-}OMe)_4]$, where $(pdt\text{-}p\text{-}OMe)^{2-}$ is 1,2-bis(*p*-anisyl)-1,2-ethylenedithiolate [36]. The resultant structure gave a 1:1 mixture of dimeric $[CoCp_2][Fe_2(pdt\text{-}p\text{-}OMe)_4]$ and monomeric $[CoCp_2][Fe(pdt\text{-}p\text{-}OMe)_2]$. This serendipitous result suggested that the weak Fe–S bridging bonds could be disrupted by crystal packing effects. The C–S and C–C distances of 1.763 and 1.373 Å indicate two closed-shell dithiolate ligands. Like the other monomeric complexes, this monoanion is perfectly square planar with the Fe ion located at the crystallographic inversion center. Density functional theoretical (DFT) calculations (using the BP86 pure functional) have shown that the lowest energy structure is that with an intermediate-spin ferric ion coordinated by two closed-shell dianionic dithiolate ligands [40]. This solution is 7 kcal/mol more favorable than the low-spin option, which although small, is a significant energy difference. Interestingly, the calculated Fe–S bond distances are in better agreement with the $S_{Fe} = 1/2$ state when comparing with the data obtained from X-ray analysis. The $S_{Fe} = 3/2$ solution gives +2.55 unpaired (Mulliken) spins on the Fe ion and +0.27 spins distributed across the four sulfurs of the two dithiolene ligands. Thus, when $[Fe^{II}(L)_2]^{2-}$ is oxidized an intermediate-spin ferric ion is generated which in turn stabilizes the iron 3d orbital manifold relative to the sulfur 3p orbitals producing more covalent Fe–S bonds. The SOMOs are still predominantly metal in character [39] and the covalency is not as large as for $[Co(L)_2]^{1-}$ [30].

A unique crystal structure of $[Per]_2[Fe(mnt)_2]$ (mnt^{2-} = maleonitrile-2,3-dithiolate) was prepared by electrochemical oxidation of perylene in a dichloromethane solution containing $[NBu_4]_2[Fe_2(mnt)_4]$ [34]. The $[Fe(mnt)_2]^{1-}$ units are well separated, with the closest distance (Fe···S) at 3.345 Å (Table 1). Also, they are perfectly square planar with Mössbauer parameters (Table 2) consistent with a central intermediate-spin Fe(III) ($S_{Fe} = 3/2$) ion. However, its temperature-dependent magnetic behavior is very similar to other dimeric dianions. This implies that one perylene is neutral and the other is a radical cation $[Per^{\bullet}]^+$.

2.2. Bis(aminothiolate)

There is just one example of a monomeric bis(aminothiolate) complex of Fe, that being $[PPh_4][Fe^{III}(tbfibt)_2]$, where $(tbfibt)^{2-}$ = 4,6-di-*tert*-butyl-2-[(pentafluorophenyl)imino]benzenethiolate (Fig. 5) [39]. The key to the isolation of a monomeric species was the pentafluorophenyl substituent of the amine, which introduces steric bulk close to the metal thus preventing dimerization. The crystal structure of the aforementioned compound consists of well separated tetraphenylphosphonium cations and $[Fe^{III}(tbfibt)_2]^{1-}$ monoanions and a solvent molecule of diethylether. The intraligand bond distances are consistent with a closed-shell iminothiolato(2-) ligands. The Fe atom rests at the crystallographic inversion center, and the two pentafluorophenyl groups are near-orthogonal (76.9°) to the planes of the five-membered chelate rings of the bis(iminobenzenethiolato)iron anion.

Table 1
Salient structural parameters for crystallographically characterized Fe bis(dithiolene) dimers.

Compound[a]	Counterion	av. Fe–S_{eq}[b]	Fe–S_{ap}[c]	Fe···Fe[d]	Pyramidal[e]	*T*, K	Ref
$[Fe^{III}_2(bdt)_4]^{2-}$	NEt_4^+	2.230	2.477	3.148	0.383	RT[f]	[48]
	$HNEt_3^+$	2.231	2.471	3.137	0.386	100	[14]
	NBu_4^+	2.230	2.424	3.036	0.418	100	[14]
$[Fe^{III}_2(tdt)_4]^{2-}$	NBu_4^+	2.220	2.513	3.252	0.384	RT	[49]
$[Fe^{III}_2(qdt)_4]^{2-}$	$AsPh_4^+$	2.234	2.488	3.194	0.344	RT	[35]
$[Fe^{III}_2(cbdt)_4]^{2-}$	NBu_4^+	2.224	2.473	3.089	0.374	150	[50]
$[Fe^{III}_2(dcbdt)_4]^{2-}$	NBu_4^+	2.225	2.476	3.114	0.368	RT	[51]
$[Fe^{III}_2(pzdt)_4]^{2-}$	NEt_4^+	2.232	2.479	3.109	0.372	100	[52]
$[Fe^{III}_2(pdt\text{-}p\text{-}OMe)_4]^{2-}$	NBu_4^+	2.216	2.474	3.091	0.451	100	[36]
$[Fe^{III}_2(mnt)_4]^{2-}$	NBu_4^+	2.225	2.474	3.079	0.361	RT	[47]
	Hpy^+[g]	2.227	2.494	3.065	0.362	RT	[53]
	$[(4\text{-}NO_2bz)py]^+$[h]	2.216	2.439	2.927	0.385	RT	[54]
	Per^+[i]	2.194	3.345	4.098	0	RT	[34]
	$FeCp^*_2{}^+$[j]	2.229	2.448	3.022	0.398	RT	[55,56]
	$CoCp_2^+$	2.226	2.496	3.094	0.360	RT	[55]
	BEDT$^+$[k]	2.224	2.477	3.043	0.362	RT	[57]
	$[Fe_2(H_2O)_2(15\text{-}C\text{-}5)]^{2+}$[l]	2.233	2.455	3.098	0.375	100	[46]
$[Fe^{III}_2(dmit)_4]^{2-}$	NBu_4^+	2.245	2.478	3.168	0.351	RT	[58]
	$FeCp^*_2{}^+$	2.238	2.500	3.166	0.359	RT	[58]
$[Fe^{III}_2(tdas)_4]^{2-}$	NEt_4^+	2.245	2.501	3.238	0.388	RT	[59]
	BEDT$^+$	2.305	2.721	3.257	0.441	RT	[60]
	BEDS$^+$[m]	2.243	2.466	3.078	0.351	RT	[61]
$[Fe^{III}_2(dmcdt)_4]^{2-}$	PPh_4^+	2.240	2.466	3.120	0.434	RT	[62]
$[Fe^{III}_2(tbbdt)_4]^{1-}$	NBu_4^+	2.230	2.424	2.851	0.423	100	[14]
$[Fe^{III}_2(pdt\text{-}p\text{-}OMe)_4]^{1-}$	NBu_4^+	2.206	2.337	2.770	0.471	100	[36]
	$CoCp_2^+$	2.207	2.328	2.744	0.491	213	[36]
$[Fe^{III}_2(pdt\text{-}p\text{-}{}^tBu)_4]^{1-}$	$CoCp_2^+$	2.207	2.348	2.804	0.478	100	[27]
$[Fe^{III}_2(tfd)_4]^{1-}$	$[Fe(\mu\text{-}SMe)_3(CO)_6]^+$[n]	2.190	2.315	2.756	0.463	RT	[63]
$[Fe^{III}_2(pdt\text{-}p\text{-}Me)_4]^0$		2.195	2.312	2.821	0.469	100	[27]
$[Fe^{III}_2(pdt\text{-}p\text{-}OMe)_4]^0$		2.198	2.335	2.792	0.490	100	[36]

[a] Ligand abbreviations available in Scheme 3.
[b] S_{eq} = equatorial sulfur stoms.
[c] S_{ap} = apical sulfur atom.
[d] Intra-iron distance.
[e] Pyramidalization is a measure of the distance of the Fe atom out of the S_4 equatorial plane.
[f] RT = room temperature (283–303 K).
[g] Hpy^+ = pyridinium.
[h] $[(4\text{-}NO_2bz)py]^+$ = 1-(4′-nitrobenzyl)pyridinium.
[i] Per^+ = perylene radical cation.
[j] $FeCp^*_2$ = decamethylferrocenium.
[k] BEDT$^+$ = bis(ethylenedithio)tetrathiafulvalene.
[l] $[Fe(H_2O)_2(15\text{-}C\text{-}5)]^{2+}$ = diaqua(1,4,7,10,13-pentaoxacyclopentadecane)iron(II).
[m] BEDS$^+$ = bis(ethylenedithio)tetraselenafulvalene.
[n] $[Fe_2(\mu\text{-}SMe)_3(CO)_6]^+$ = tri-μ-methylthio-hexacarbonyldiiron(II).

This paramagnetic species exhibited a rhombic X-band EPR spectrum that was simulated considering a 3:2 ratio of two isomers (*a* and *b*) with g_a = (3.14, 4.90, 1.90) and g_b = (3.36, 482, 1.99): the *cis* and *trans* isomers of this monoanion. A large zero-field splitting (D = +18.0 cm^{-1}) and rhombicity (E/D = 0.19) were derived from the simulation, similar to the values obtained for $[NBu_4][Fe^{III}(qdt)_2]$ [39]. The compound has a room temperature magnetic moment of 3.85 μ_B consistent with an intermediate-spin Fe(III) ion and S_t = 3/2 ground state. The Mössbauer spectrum exhibits of a single quadrupole doublet with an isomer shift δ = 0.23 mm s^{-1} and an enormous quadrupole splitting ΔE_Q = 4.55 mm s^{-1}. The qualitative bonding scheme displayed in Fig. 6 shows three singly occupied metal *d* orbitals, one doubly occupied *d* orbital, and one *d* orbital is empty. This is the hallmark of intermediate-spin Fe(III) and the Mulliken spin density plot localizes three unpaired electrons at the ferric ion (Fig. 6). Interestingly, the Fe composition of the SOMOs is slightly less than those of intermediate-spin Fe(II) dianionic complexes due to increased Fe–S covalency. This electronic structure description parallels that for $[NBu_4][Fe^{III}(qdt)_2]$ described above.

3. Dinuclear complexes

3.1. Bis(dithiolene)

3.1.1. Synthesis and structural overview

In 1963 [5], the reaction of ferrous chloride and toluene-3,4-dithiolate$(tdt)^{2-}$, with the addition of tetraphenylarsonium chloride yielded the first bis(dithiolene)iron complex, formulated as $[AsPh_4][Fe(tdt)_2]$. Gray et al. proposed a high-spin Fe(I) d^7 (S_{Fe} = 3/2) central ion given a room temperature effective magnetic moment of 4.39 μ_B, implying two open-shell $(tdt^{\bullet})^{1-}$ π radical ligands. At almost the same time, Weiher et al. combined $FeCl_3{\cdot}6H_2O$ with $Na_2(mnt)$ and $[NEt_4]Cl$ in ethanol to give $[NEt_4][Fe(mnt)_2]$ [41]. The magnetic susceptibility at room temperature corresponded to ∼1.6 μ_B, consistent with S_t = 1/2, is provided by a low-spin ferric ion coordinated by two closed-shell mnt^{2-} ligands. An alternative synthetic pathway was used to prepare the first neutral iron bis(dithiolene), $[Fe(tfd)_2]$ (tfd^{2-} = bis(trifluoromethyl)ethylenedithiolate), via the reaction of

Table 2
Experimental Mössbauer spectral parameters for monomeric and dimeric homoleptic iron bis(dithiolene) complexes at 80 K.

Compound[a]	Counterion	δ[b]	ΔE_Q[c]	S_{Fe}[d]	S_t[e]	Ref
$[Fe^{II}(dtsq)_2]^{2-}$	PPh_4^+	0.66	−3.97	2	2	[28]
$[Fe^{II}(bdt)_2]^{2-}$	NMe_4^+	0.44	1.16	1	1	[32]
	$NHEt_3^+$	0.44	1.19	1	1	[30]
	NBu_4^+	0.46	1.08	1	1	[30]
$[Fe^{III}(qdt)_2]^{1-}$	NBu_4^+	0.37	3.02	3/2	3/2	[39]
$[Fe^{III}{}_2(bdt)_4]^{2-}$	NBu_4^+	0.31	2.95	3/2	0	[48]
$[Fe^{III}{}_2(tdt)_4]^{2-}$	NBu_4^+	0.34	2.95	3/2	0	[69]
$[Fe^{III}{}_2(tbbdt)_4]^{2-}$	NBu_4^+	0.36	2.87	3/2	0	[14]
$[Fe^{III}{}_2(Cl_4\text{-}bdt)_4]^{2-}$	NBu_4^+	0.32	3.02	3/2	0	[69]
$[Fe^{III}{}_2(qdt)_4]^{2-}$	$PMePh_3^+$	0.34	3.33	3/2	0	[71]
	PPh_4^+	0.35	3.31	3/2	0	[39]
$[Fe^{III}{}_2(cbdt)_4]^{2-}$[f]	NBu_4^+	0.34	3.01	3/2	0	[50]
$[Fe^{III}{}_2(dcbdt)_4]^{2-}$	NBu_4^+	0.32	3.01	3/2	0	[51]
$[Fe^{III}{}_2(pdt)_4]^{2-}$	NEt_4^+	0.35	2.37	3/2	0	[69,70]
$[Fe^{III}{}_2(pdt\text{-}p\text{-}^tBu)_4]^{2-}$	Cp_2Co^+	0.36	2.26	3/2	0	[27]
$[Fe^{III}{}_2(tfd)_4]^{2-}$	NEt_4^+	0.33	2.50	3/2	0	[69]
$[Fe^{III}{}_2(mnt)_4]^{2-}$	NEt_4^+	0.33	2.76	3/2	0	[69,70,72]
	NBu_4^+	0.33	2.68	3/2	0	[34]
	Hpy^+	0.35	2.69	3/2	0	[53]
	Per^+	0.34	2.79	3/2	0	[34]
	$FeCp^*{}_2^+$	0.34	2.64	3/2	0	[56]
$[Fe^{III}{}_2(dmit)_4]^{2-}$	NBu_4^+	0.36	2.58	3/2	0	[51]
$[Fe^{III}{}_2(tbbdt)_4]^{1-}$	NBu_4^+	0.28	2.70	3/2	1/2	[14]
$[Fe^{III}{}_2(pdt\text{-}p\text{-}^tBu)_4]^{1-}$	$CoCp_2^+$	0.29	2.13	3/2	1/2	[27]
$[Fe^{III}{}_2(Cl_4\text{-}bdt)_4]^0$		0.32	3.15	3/2	0	[69]
$[Fe^{III}{}_2(pdt)_4]^0$		0.25	2.01	3/2	0	[69]
$[Fe^{III}{}_2(pdt\text{-}p\text{-}Me)_4]^0$		0.26	2.18	3/2	0	[27]
$[Fe^{III}{}_2(pdt\text{-}p\text{-}^tBu)_4]^0$		0.25	1.93	3/2	0	[27]
$[Fe^{III}{}_2(tfd)_4]^0$		0.25	2.39	3/2	0	[69]

[a] Ligand abbreviations available in Scheme 3.
[b] Isomer shift, mm s^{-1}.
[c] Quadrupole splitting, mm s^{-1}. The sign is unknown unless determined by an applied-field measurement.
[d] Intrinsic iron spin state.
[e] Total spin ground state of the complex.
[f] Spectrum recorded at 4.2 K.

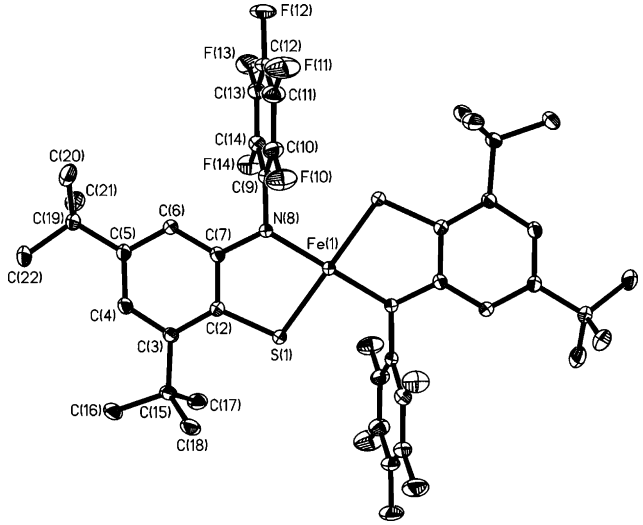

Fig. 5. Crystal structure of the monoanion in $[PPh_4][Fe(tbfibt)_2]$ [39].

$Fe(CO)_5$ and bis(trifluoromethyl)-1,2-dithietene [42]. In the same publication, Holm and co-workers also isolated the monoanion $[NEt_4][Fe(tfd)_2]$. The monoanionic complex with an $S_t = 1/2$ ground state did not yield an EPR signal at temperatures approaching 100 K. The field was first alerted to the possible dimerization of two monoanionic units with the crystallographic characterization of $[Co_2(tfd)_4]$ that showed a dimeric structure, with the planar $[Co(tfd)_2]^{1-}$ units linked by reasonably robust Co–S bonds at 2.382 Å [43]. The dimeric nature of Fe bis(dithiolene) complexes was inferred by Balch and Holm [44], noticing that $[Fe_2(tfd)_4]$ was isomorphous to the Co species. Moreover, these Co and Fe complexes possessed similar electron transfer behavior, and they proceeded to isolate $[NEt_4][Fe_2(tfd)_4]$ and $[NEt_4]_2[Fe_2(tfd)_4]$. Interestingly, magnetic susceptibility data showed these neutral, monoanionic, and dianionic dimers have room temperature magnetic moments of 1.59, 2.08 and 1.39 μ_B, for what are considered $S_t = 0$, $S_t = 1/2$, and $S_t = 0$ compounds, respectively.

A different synthetic approach to manufacturing dithiolene ligands employed by Schrauzer et al. afforded the first neutral iron bis(dithiolene) complexes [45]. The procedure involves reacting benzoin (an α-hydroxyketone collectively known as acyloins) with phosphorus pentasulfide in a high boiling point solvent, such as dioxane or xylene. The reaction produces *in situ* a dithiophosphoric ester that readily reacts with metal chlorides to afford metal dithiolene complexes (Scheme 5). The electrochemistry of

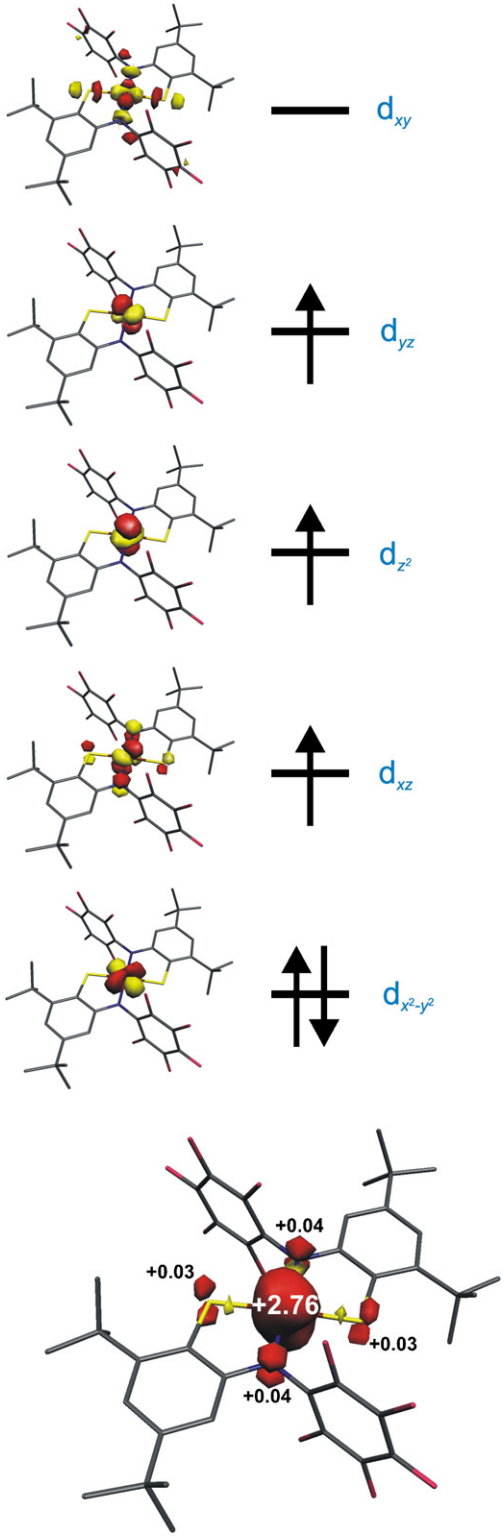

Fig. 6. Qualitative MO manifold and Mulliken spin density plot for $[Fe(tbfibt)_2]^{1-}$ [39].

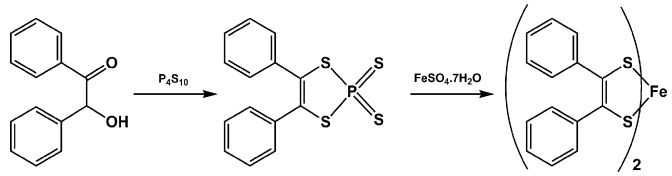

Scheme 5. Ref. [45].

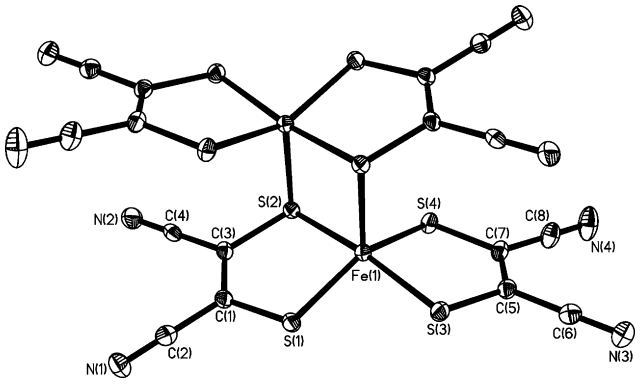

Fig. 7. Crystal structure of the dianionic complex $[Fe_2(mnt)_4]^{2-}$ [46].

$[Fe_2(pdt)_4]$ (pdt^{2-} = 1,2-diphenyl-1,2-ethylenedithiolate) showed four reversible reduction processes, similar to $[Fe_2(tfd)_4]$. The neutral species was chemically reduced using one and two equivalents of anhydrous hydrazine to give $[AsPh_4][Fe_2(pdt)_4]$ and $[AsPh_4]_2[Fe_2(pdt)_4]$, respectively. The former was classified as diamagnetic following the Gouy method.

Crystallographic characterization of centrosymmetric $[NBu_4]_2[Fe_2(mnt)_4]$ in 1967 confirmed the suspected dimeric nature of these compounds [47], with each Fe ion bound by five sulfur atoms that rest at the vertices of a square pyramid (Fig. 7). The apical Fe–S bond is longer (2.474 Å) than the equatorial Fe–S bonds (avg. 2.223 Å) to the two $(mnt)^{2-}$ ligands. The Fe atom is positioned 0.36 Å out of the equatorial plane and the Fe···Fe distance of 3.079 Å is out of the range for a metal–metal bond. These are the salient structural features synonymous with all $[Fe_2(L)_4]^{2-}$ (Table 1).

Alvarez and Hoffmann provided an elegant account for the observed dimerization in Fe and Co bis(dithiolene) complexes [64]. Unlike the Group 10 metals Pd and Pt, where the dimerization occurs though metal–metal bonds, for the smaller Fe atom, bonding occurs between the d_{z^2} and the S $3p_z$ orbitals that produces two bonding and two antibonding molecular orbitals. For d^8 systems, the antibonding levels are filled to give a net repulsive interaction, however, these levels are empty for Fe(III) d^5 (generally accepted to be the Fe oxidation state in dianionic dimers) creating the stabilizing bond. Additionally, the Fe atom is lifted out of the bis(dithiolene) equatorial plane to minimize inter-ring repulsion between the adjacent metallodithiolene π layers. The structural data presented in Table 1 shows a consistent pyramidalization of the Fe ion that increases upon oxidation of the dimer from a dianion to a neutral species. This in turn shortens the Fe···Fe distance to ~2.8 Å for the neutral complexes, though this is not regarded as a metal–metal bond. Eisenberg [63], in his light-hearted and rather amusing account of the 2-year crystallographic determination of $[Fe_2(\mu\text{-}SMe)_3(CO)_6][Fe_2(tfd)_4]$, suggested a decrease in the electron density in the vicinity of the Fe ion in systems containing strong π acid ligands, such as $(tfd)^{2-}$, increases the metal–metal interaction in more oxidized species.

More noteworthy are the intraligand distances that change dramatically across electron transfer series, $[Fe_2(pdt\text{-}p\text{-}OMe)_4]^z$ (z = 0, 1−, 2−), shown in Scheme 6. Each member was very recently crystallographically characterized (Fig. 8) [36]. For the dianion, the C–S and C–C bond distances of 1.768 and 1.352 Å clearly indicate closed-shell, dianionic dithiolate ligands. One-electron oxidation leads to a slight shortening of all five Fe–S bonds, and more importantly, the C–S bonds of the *terminal* dithiolene ligand shorten to 1.725 Å and the C–C bonds lengthen to 1.378 Å. The same bonds for the *bridging* dithiolene remain essentially unchanged. This effect is amplified in the neutral compound, $[Fe_2(pdt\text{-}p\text{-}OMe)_4]$, where the bridging dithiolene ligands have C–S at 1.753 Å C–C at 1.371 Å indicative of

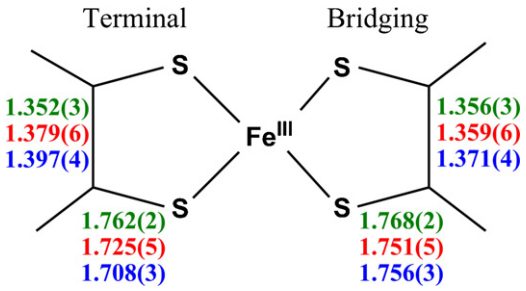

Scheme 6. Variation of the intraligand bond distances (Å) in the $[Fe(pdt\text{-}p\text{-}OMe)_4]^z$ ($z = 0$, blue; 1−, red; 2−, green) series [36].

dianionic dithiolates, while the terminal dithiolenes have short C–S (1.708 Å) and long C–C (1.397 Å) bonds representative of monoanionic π radical ligands.

While metathesis is the most common method for appending dithiolenes to iron, one additional route has been developed. The activated acetylene, dimethylacetylene dicarboxylate is reacted with $[PPh_4]_2[Fe_2S_{12}]$ to give $[PPh_4]_2[Fe_2(dmcdt)_4]$ ($dmcdt^{2-}$ = dimethyldicarboxyethylenedithiolate) [62]. Schrauzer reported reactions of $Fe(CO)_5$ or $Fe_3(CO)_{12}$ with diphenylacetylene and elemental sulfur that yielded $[Fe_2(\mu\text{-}S)_2(pdt)_2]$, rather than a homoleptic complex, as in the case for nickel [45].

3.1.2. Electronic structure

It was shown early on that Fe bis(dithiolene) complexes form a four-membered electron transfer series [4,44,45]. Air-sensitive, monomeric $[Fe^{II}(L)_2]^{2-}$ is readily oxidized in air to give the dianionic dimer. The process can be reversed: a black-red solution of $[Fe^{III}{}_2(bdt)_4]^{2-}$ combined with sodium borohydride produces a red-yellow solution of the monomer, which was isolated in 26% yield [32]. Sawyer et al. presented a detailed discussion on whether this two-electron oxidation was metal- or ligand-centered [49]; ultimately favoring the latter and formulated the product as $[Fe^{II}{}_2(tdt)_2(tdt^{\bullet})_2]^{2-}$. It became apparent later on with a high-quality X-ray crystal structure of $[NBu_4]_2[Fe_2(bdt)_4]$ at 100 K that the intraligand bond distances consistent with closed-shell $(bdt)^{2-}$ ligands coordinated to two ferric ions [14], which is the general consensus derived from crystallographic, magnetic and spectroscopic analysis for other systems. It should be noted that complexes with $(mnt)^{2-}$ are the most abundantly studied and characterized, and

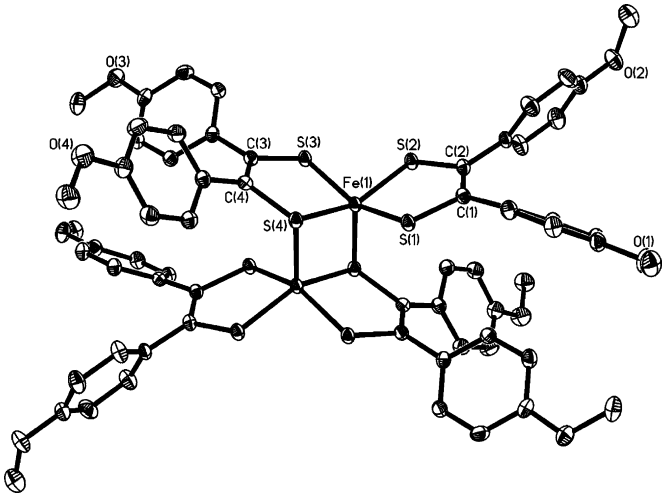

Fig. 8. Crystal structure of the neutral complex $[Fe_2(pdt\text{-}p\text{-}OMe)_4]$ that is representative of the monoanion and dianion members of this electron transfer series [36].

the extensive delocalization throughout this ligand renders an oxidation state assignment near-impossible. The clearest example of this can be seen comparing $[Ni(mnt)_2]^{1-}$ and $[Ni(mnt)_2]^{2-}$ [65], which show no change in the intraligand bond distances despite ligand oxidation in the former [66].

The spin state of the ferric ion has been a more debated topic in the literature; both intermediate-spin ($S_{Fe} = 3/2$) and low-spin ($S_{Fe} = 1/2$) states have been considered. Variable-temperature magnetic susceptibility data for a number of different $[Fe_2(L)_4]^{2-}$ salts has been successfully modeled assuming intramolecular antiferromagnetic coupling between the ferric ions [14,27,34,39,48,50,53,54,60]. Dance was the first to include a necessary second paramagnetic state to adequately fit the magnetic data at higher temperatures. This excluded the possibility of a very strong interaction between the mononuclear subunits, like an Fe–Fe bond, that would give each a doublet spin state [67]. For all but two [51,56], the best fit was obtained for two intermediate-spin ($S_{Fe} = 3/2$) ions; the coupling affords the $S_t = 0$ ground state. The coupling values, J, range from −80 to $-300\,cm^{-1}$, depending on the dithiolene ligand. The magnetic susceptibility data of $[Fe_2(dcbdt)_4]^{2-}$ ($dcbdt^{2-}$ = 4,5-dicyanobenzene-1,2-dithiolate) afforded a slightly better fit assuming two antiferromagnetically coupled low-spin ($S_{Fe} = 1/2$) ferric ions [51]. Considering the structural data shown in Table 1, it is not entirely clear why this is the case, though a very unique dimeric structure was obtained for the analogous nickel salt $[NBu_4]_2[Ni_2(dcbdt)_4]$ [68]. Mössbauer spectroscopy has been particularly useful for gauging the iron oxidation and spin state. The Mössbauer parameters recorded at 80 K for a large number of dimeric dianions are listed in Table 2 and show the range for the isomer shift is 0.31–0.36 mm s^{-1} and quadrupole splitting 2.26–3.31 mm s^{-1} [14,27,34,39,48,50,51,53,56,69–71]. These parameters are the same as those for mononuclear $[NBu_4][Fe^{III}(qdt)_2]$ [39], and clearly indicate two intermediate-spin Fe(III) ($S_{Fe} = 3/2$) ions that antiferromagnetically couple to give the $S_t = 0$ ground state. Larger quadrupole splittings occur for complexes with aromatic-1,2-dithiolate ligands; and increase with increasing electron withdrawing nature of the substituent. The "olefinic" dithiolenes, those with a genuine carbon–carbon double bond [6], show the same substituent trend and are overall smaller than their aromatic dithiolate counterparts. The large quadrupole splitting seen for $[NBu_4]_2[Fe_2(dcbdt)_4]$ suggests that it has intermediate-spin ferric ions rather than low-spin ferric ions, in accordance with simple ligand field theory.

Dimeric dianions have been used as counteranions in charge transfer salts, particularly $[Fe_2(mnt)_4]^{2-}$ [34,50,51,53,54,56,58,60,61]. Here, bis(dithiolene) salts are incorporated due to their planar structure, extensive π orbital system of the metallodithiolene ring that forms stable ion-radical species at various potentials, and intramolecular antiferromagnetic interactions. A thorough overview of the properties and uses of these materials has been collated by Faulmann and Cassoux [73].

The electronic structure of the more oxidized members of the electron transfer series (monoanion, neutral, monocation) had, until very recently, been ignored. One-electron oxidation of $[Fe^{III}{}_2(L)_4]^{2-}$ leads to a $S_t = 1/2$ monoanionic dimer, $[Fe_2(L)_4]^{1-}$ [27], where formal oxidation states of +III and +IV can be assigned to the iron centers. Further oxidation gives formally the neutral Fe(IV)/Fe(IV) compound, and in some cases, this neutral species can be reversibly one-electron oxidized to the monocationic dimer, formally Fe(IV)/Fe(V). The possibility of stabilizing high-valent iron must be questioned in systems containing redox active dithiolene ligands. Certainly there is every indication from X-ray crystallography that the ligands are oxidized, clearly evident from an analysis of the intraligand bond distances in the $[Fe_2(pdt\text{-}p\text{-}OMe)_4]^z$ ($z = 0$, 1−, 2−) series (Scheme 6) [36].

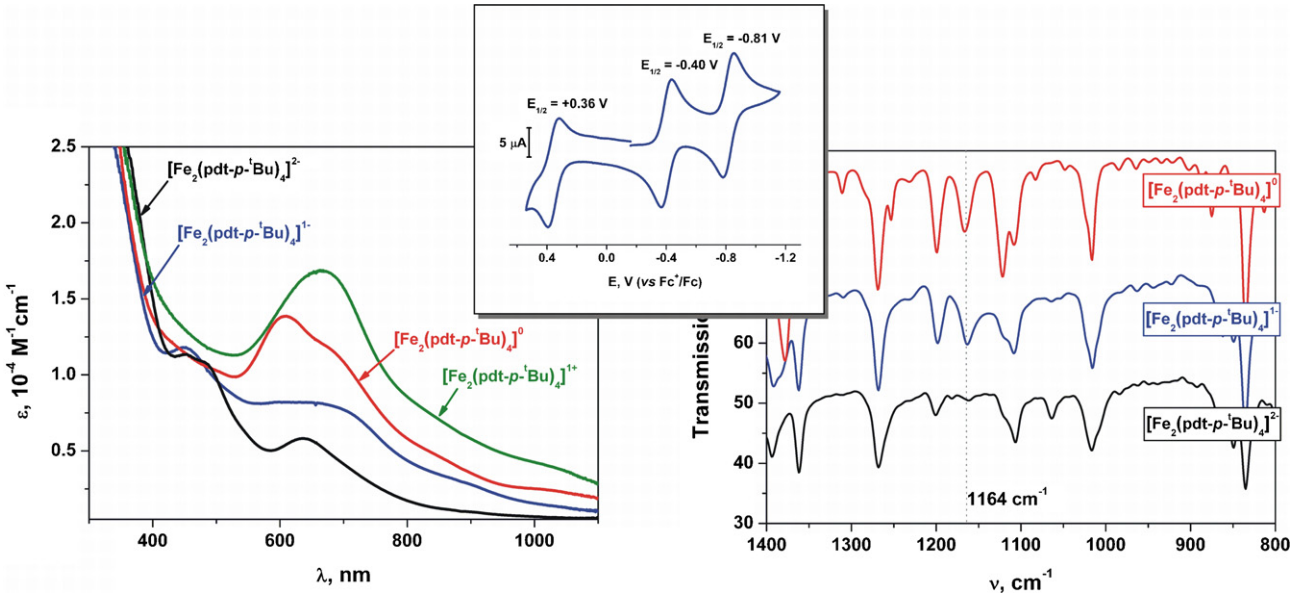

Fig. 9. Electronic absorption spectra, cyclic voltammogram and IR spectra for the $[Fe^{III}_2(pdt\text{-}p\text{-}^tBu)_4]^z$ ($z = 1+, 0, 1-, 2-$) electron transfer series [27]. The dotted line indicates the presence (and absence) of a ν(C=S•) stretching frequency.

The cyclic voltammogram of the $[Fe_2(pdt\text{-}p\text{-}^tBu)_4]^z$ ($z = 1+, 0, 1-, 2-$) electron transfer series is shown in Fig. 9, along with the electronic absorption and infrared spectra [27]. These spectroscopic methods are used to diagnose the presence of ligand π radicals [15], and these radical fingerprints are clearly evident in this electron transfer series. Firstly, there is an increase in the intensity of the charge transfer band at ~650 nm as the dianionic compound is oxidized through to the monocationic dimer. Secondly, the infrared spectrum of the monoanion and neutral compounds exhibit a new feature at 1164 cm^{-1} that has been assigned to the C=S• stretching frequency [13]; it is noticeably absent in the spectrum of the dianion. Zero-field Mössbauer spectroscopy assesses the other redox active site in the complex: the iron ion. Mössbauer spectra of the monoanionic dimers, $[Fe_2(L)_4]^{1-}$ [14,27], exhibit only a single quadrupole doublet which rules out a metal-centered oxidation to give a $Fe^{III}Fe^{IV}$ mixed valent species and indicates ligand mixed valency of class II or III on the timescale of the Mössbauer experiment (Fig. 10). The isomer shift and quadrupole splitting both decrease consistent with a weakening of the ligand field provided by the coordinated π radical that increases the effective nuclear charge of the iron ion. Further ligand-centered oxidation to neutral $[Fe_2(L)_4]$ leads to a further decrease in the isomer shift and quadrupole splitting with the sole exception of $[Fe_2(Cl_4\text{-}bdt)_4]^0$ [69].

The spectroscopic data clearly show that the intrinsic oxidation state of the iron ion remains +III in an intermediate-spin ($S_{Fe} = 3/2$) state, and therefore this electron transfer series is connect by reversible ligand-centered redox processes (Scheme 7). By crystallography [14,27,36,63], we can identify the terminal dithiolene ligand as the oxidized entity, since the bridging ligand with three-coordinate sulfur (thioether character) is more difficult to oxidize. The oxidation of the dithiolene to a π radical monoanionic ligand increases the π acidity of this species, which as noted by Eisenberg [63], removes electron density away from ferric ion and lowers the isomer shift. The temperature dependence of the magnetic moments for the neutral, monoanionic and dianionic dimers have been successfully modeled assuming two antiferromagnetically intermediate-spin Fe(III) ($S_{Fe} = 3/2$) ions with coupling values, J_{Fe1Fe2}, ranging −250 to −200 cm^{-1}, and for the monoanion and neutral species, metal–radical ligand couplings of −140 and −200 cm^{-1}, respectively [27]. The $S_t = 1/2$ ground state of $[Fe_2(pdt\text{-}p\text{-}Me)_4]^{1-}$ was established with $\mu_{eff} = 1.8\ \mu_B$ at 4.2 K.

Broken symmetry DFT calculations on this electron transfer series (1+ → 2−)[74] gratifyingly show three α-spins (spin up) at one Fe ion, and three β-spins (spin down) at the other in the Mulliken spin density plot (Fig. 11). This is the hallmark for two antiferromagnetically coupled intermediate-spin ferric ions. For $[Fe_2(pdt\text{-}p\text{-}Me)_4]^{2-}$, slightly less than three spins are located at the ferric ion in the due to covalent Fe–S bonds that deposit spin density on the sulfur atoms of the first coordination sphere. This contrasts the spin density distribution for $[Fe^{II}(bdt)_2]^{2-}$, where the unpaired spins are entirely localized on the metal. Oxidation of one terminal dithiolene ligand sees +0.71 spins localized there, consistent with the electronic structure defined spectroscopically. This trend continues for the neutral, where spin density is seen on the other terminal dithiolene, and the monocation, where a bridging ligand is now oxidized.

3.2. Bis(aminothiolate)

3.2.1. Synthesis and molecular and electronic structures

Preparation of iron aminothiolate compounds developed along side analogous dithiolene chemistry because it was shown that these entities undergo facile one-electron transfer reactions [17]. However, there is a dearth of isolated and structurally characterized of homoleptic bis(aminothiolate) compounds essentially due to the profound insolubility of compounds with the commercially available aminobenzenethiolate ligand [75]. There are many examples of aminobenzenethiolate units in large polydentate ligands where coordinating units have been appended to the amino group that will not feature in this discussion [18].

The original paper in this field by Larkworthy et al. presented the reaction of aminobenzenethiol with ferrous sulfate in the presence of sodium hydroxide and sodium acetate to produce the pale yellow $[Fe(abt)_2]$ [75]. A less than stoichiometric quantity of hydroxide was used to prevent rust formation (hydrated oxides of iron). Attempts to prepare a ferric complex failed because the ligand was routinely oxidized to the dimeric disulfide-bridged $(abt)_2$. $[Fe^{II}(abt)_2]$, as it was then formulated, exhibited an effective magnetic moment of 3.95 μ_B at 308 K. This low moment was caused by large antiferromagnetic exchange coupling between two high-spin Fe(II) ($S_{Fe} = 2$)

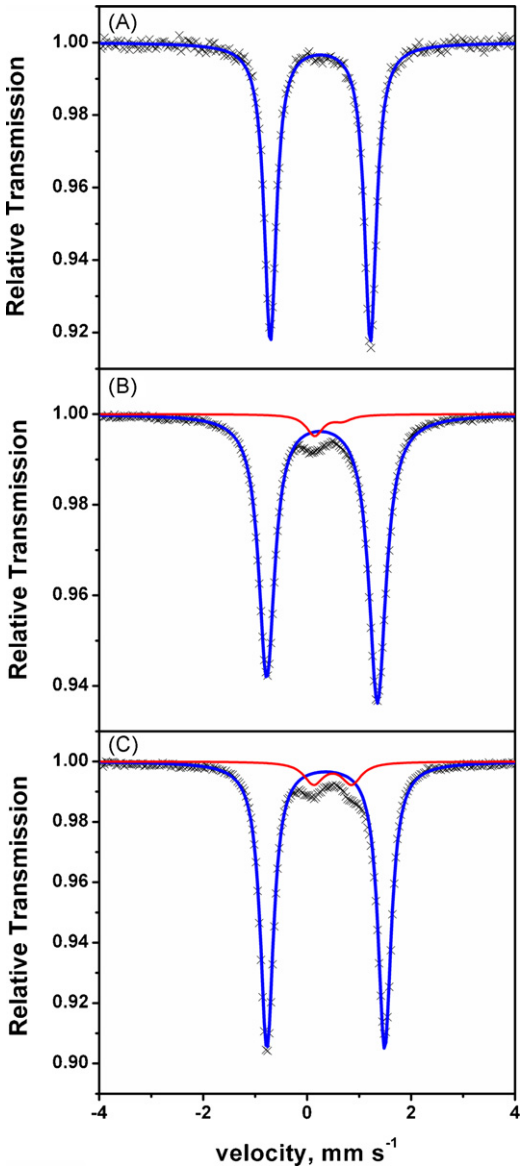

Fig. 10. Mössbauer spectra of $[Fe^{III}_2(L)_4]^{2-}$ (A), $[Fe^{III}_2(L^{\bullet})(L)_3]^{1-}$ (B), and $[Fe^{III}_2(L^{\bullet})_2(L)_2]^{0}$ (C), where L = (pdt-*p*-^{t}Bu)$^{2-}$, recorded at 80 K [27].

ions and, based on its poor solubility and the spectroscopy, it was proposed this isolated compound was a sulfur-bridged six-coordinate polymer.

In 2003, preparation and crystallographic characterization of (μ-S,S)$[Fe^{II}(tbabt)_2]_2$ [25], with the more soluble *tert*-butyl-substituted aminobenzenethiolate ligand $(tbabt)^{1-}$ [76], confirmed a dimeric structure where the planar monomeric units are connected by Fe–S bonds. The intraligand bond distances were consistent with four $(tbabt)^{1-}$ ligands bound to two ferrous ions to account for the overall neutral charge. The single quadrupole

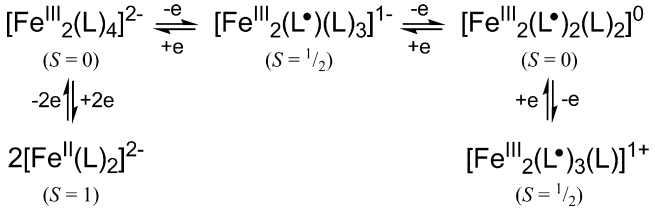

Scheme 7. Refs. [14,27].

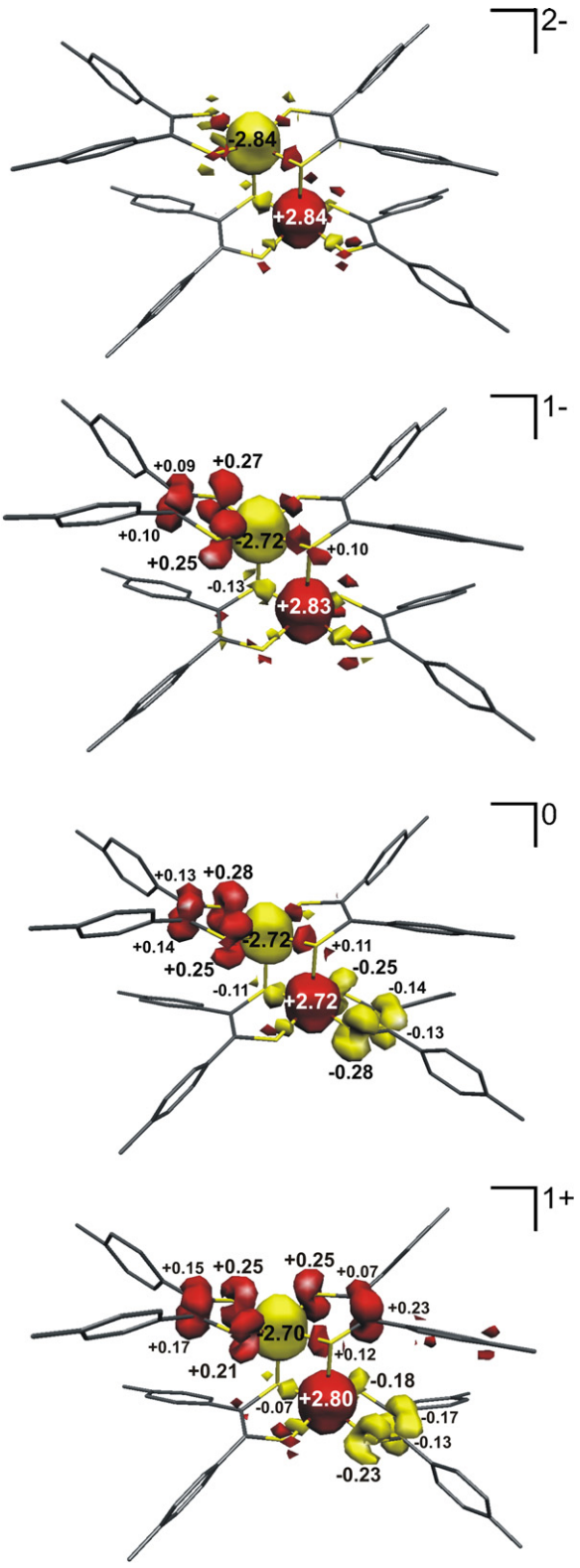

Fig. 11. Mulliken spin density plots for the $[Fe^{III}_2(L)_4]^z$ (z = 1+, 0, 1−, 2−; L = pdt-*p*-Me^{2-}) from dianion (top) to monocation (bottom) (red: α-spin; yellow: β-spin) [74].

Table 3
Experimental Mössbauer spectral parameters for homoleptic iron bis(aminothiolate) dimers at 80 K.

Compound[a]	δ[b]	ΔE_Q[c]	S_{Fe}[d]	Ref
(μ-S,S)[Fe^{II}(abt)$_2$]$_2$	0.91	4.10	2	[25]
(μ-S,S)[Fe^{II}(tbabt)$_2$]$_2$	0.88	3.68	2	[25]
(μ-NH,NH)[Fe^{III}(tbibt)(tbabt)]$_2$	0.33	2.83[e]	3/2	[25,77]
(μ-S,S)[Fe^{III}(tbibt)(tbabt)]$_2$	0.30	2.71	3/2	[25]
(μ-NH,NH)[Fe^{III}(tbibt)(tbitbs$^{\bullet}$)]$_2$	0.20	2.67	3/2	[26]
(μ-S,S)[Fe^{III}(tbibt)(tbitbs$^{\bullet}$)]$_2$	0.17	2.73	3/2	[26]
(μ-S,S)[Fe^{II}(bmae)]$_2$	0.87	3.24	2	[25]
(μ-S,S)[Fe^{III}(bmae$^{\bullet}$)]$_2$	0.16	2.68	3/2	[26]
	0.25	2.06	3/2	

[a] Ligand abbreviations available in Scheme 4.
[b] Isomer shift, mm s^{-1}.
[c] Quadrupole splitting, mm s^{-1}. The sign is unknown unless determined by an applied-field measurement.
[d] Intrinsic iron spin state.
[e] The published quadrupole splitting is erroneous.

doublet in the Mössbauer spectra of (μ-S,S)[Fe^{II}(abt)$_2$]$_2$ and (μ-S,S)[Fe^{II}(tbabt)$_2$]$_2$ have δ = 0.91 and 0.85 mm s^{-1} and ΔE_Q = 4.10 and 3.68 mm s^{-1}, respectively, which are classic values for high-spin ferrous (Table 3). The magnetic data (4–300 K) of (μ-S,S)[Fe(abt)$_2$]$_2$ was refitted for $S_{Fe1} = S_{Fe2} = 2$ ($S_t = 0$) that gave an exchange coupling of $J = -47 \pm 4$ cm^{-1} and zero-field splitting of $|D_1| = |D_2| = 10 \pm 5$ cm^{-1}.

The yellow high-spin ferrous complexes are very air-sensitive, and exposure to dioxygen in the solution and solid state results in dark, usually black powders, that had not until recently been characterized [25,26,75]. In an attempt to produce a ferric species [25], a mixture of aminobenzenethiol and $FeCl_2 \cdot 4H_2O$ was stirred with triethylamine in aerated tetrahydrofuran, however, the resultant yellow-green crystals isolated in 70% yield were that of [PPh_4][Fe^{II}(abt)$_2$(itbs$^{\bullet}$)]—a five-coordinate iron salt with an apical iminothionebenzosemiquinone radical ligand (itbs$^{\bullet}$)$^{1-}$. The redox level of the ligands is clearly established from the X-ray structure: two (abt)$^{1-}$ ligands with C–S and C–N bond distances of 1.762 and 1.444 Å, respectively, with the apical (itbs$^{\bullet}$)$^{1-}$ ligand has a short C–S bond at 1.747 Å and a very short C–N bond at 1.356 Å. These values are in agreement with the known intraligand distances for the various redox levels on aminothiolates derived from crystallographic studies (Scheme 8) [78]. Its Mössbauer spectrum consists of a 1:1 mixture of two quadrupole doublets, with δ = 0.92 and 0.88 mm s^{-1}, and ΔE_Q = 4.05 and 3.38 mm s^{-1}, respectively, which indicates two structurally slightly different high-spin Fe(II) ($S = 2$) ions due to two different conformations of the apical (itbs$^{\bullet}$)$^{1-}$ ligand. An effective magnetic moment, μ_{eff} ~4.2 μ_B corresponds to a $S_t = 3/2$ ground state, generated by the antiferromagnetic coupling of the ligand radical ($S_L = 1/2$) with the high-spin Fe(II) center. The coupling was estimated at $J = -135 \pm 25$ cm^{-1}.

A similar procedure was followed using the more soluble *tert*-butyl-substituted (tbabt)$^{1-}$ ligand [25], which resulted in a brown precipitate. Its structural characterization identified this as the oxidized dimer, (μ-NH,NH)[Fe^{III}(tbibt)(tbabt)]$_2$, where the bridge is an Fe–N bond. The terminal (tbabt)$^{1-}$ ligands are characterized by C–S and C–N bond lengths of 1.771 and 1.458 Å, respectively, while the more electron rich and consequently bridging 4,6-di-*tert*-butyliminobenzenethiolate (tbibt)$^{2-}$ ligands have the same C–S distance with a noticeably shorter C–N bond (1.423 Å). The protonation and oxidation level of the ligands are distinguished by IR spectroscopy, with the assignment of ν_{as}, $\nu_s(NH_2)$ and ν(N–H) stretching vibrations. Interestingly, the same reaction carried out with lithium methoxide as base, afforded (μ-S,S)[Fe^{III}(tbibt)(tbabt)]$_2$. These isomers are discriminated by their electronic absorption spectra, with a slight blue-shift in the latter. The Mössbauer spectral parameters show a clear change in the iron oxidation state. Isomer shifts of 0.33 and 0.30 mm s^{-1} and quadrupole splittings of 2.83 [77] and 2.71 mm s^{-1} for the (μ-NH,NH) and (μ-S,S) compounds, respectively, are indicative of intermediate-spin Fe(III) ($S_{Fe} = 3/2$) ions, as outlined for the bis(dithiolene) analogues.

Dichloromethane solutions of the [Fe^{III}(tbibt)(tbabt)]$_2$ isomers are sensitive to oxygen; brown solutions transform into dark-blue solutions that upon addition of hexane, yielded dark brown-black crystals in excellent yields [26]. Both isomers have been structurally characterized, and compared to the [Fe^{III}(tbibt)(tbabt)]$_2$ precursors, the terminal (tbabt)$^{1-}$ ligands have been oxidized that sees the C–S and C–N bond distances shorten to 1.742 and 1.386 Å for the μ-NH,NH isomer, and 1.727 and 1.360 Å for the μ-S,S isomer, respectively (Fig. 12). Additionally, there is a quinoidal distortion of the aromatic ring, with four long and two short C–C bonds. These oxidized products are formulated as (μ-

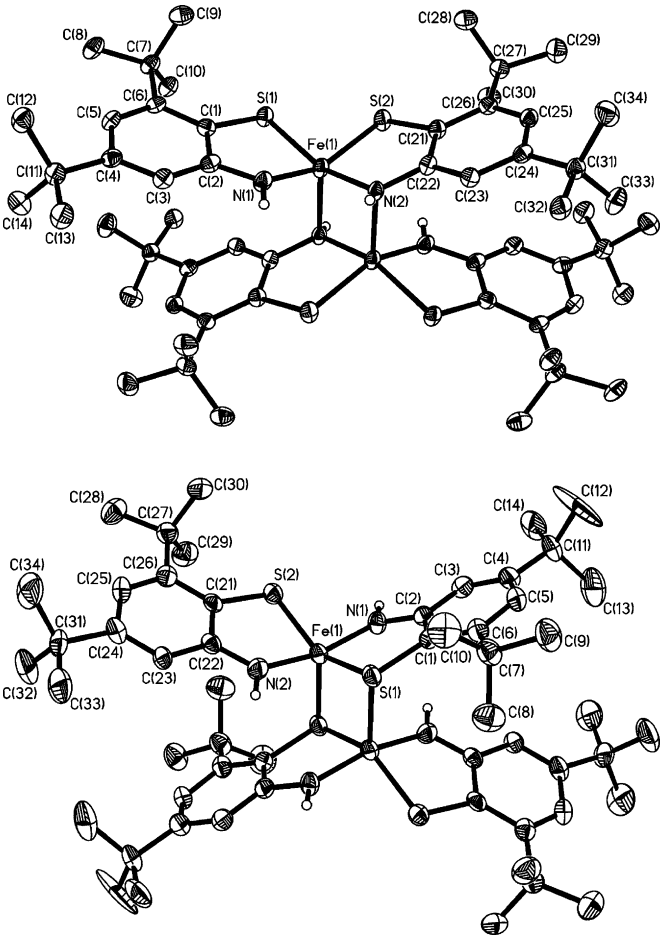

Fig. 12. X-ray crystallographic structures of the two isomers (μ-NH,NH)[Fe^{III}(tbibt)(tbitbs$^{\bullet}$)]$_2$ (top) and (μ-S,S)[Fe^{III}(tbibt)(tbitbs$^{\bullet}$)]$_2$ (bottom) [26].

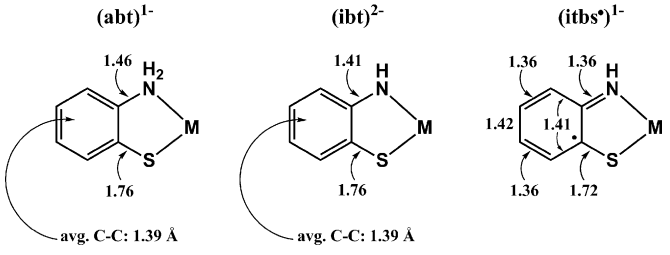

Scheme 8. Bond distances (Å) in aminothiolate ligands [78].

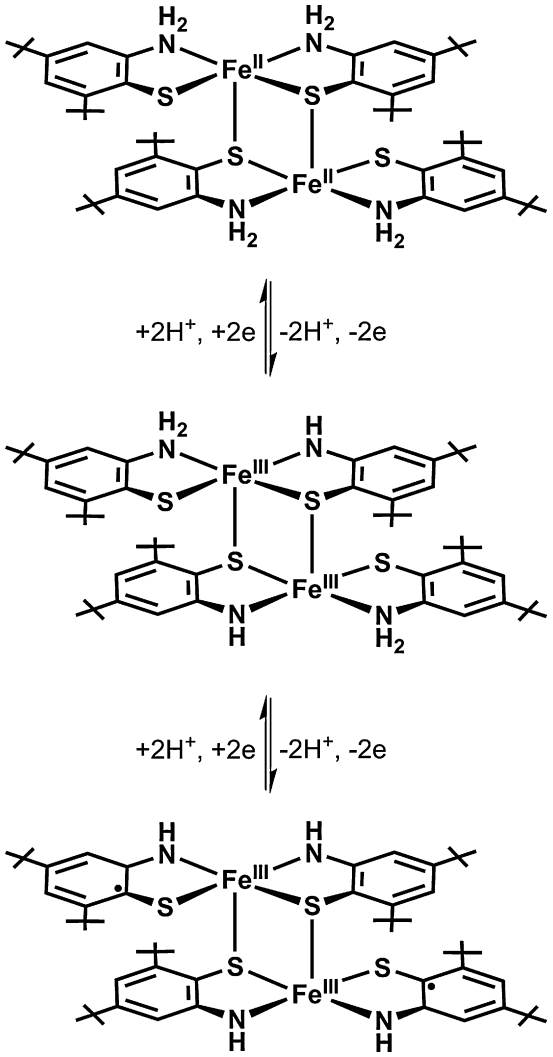

Scheme 9. Refs. [25,26].

NH,NH)[Fe^{III}(tbibt)(tbitbs•)]$_2$ and (μ-S,S)[Fe^{III}(tbibt)(tbitbs•)]$_2$ and represent the highest oxidation level for this three-membered proton–electron transfer series, as shown in Scheme 9. The near-black color of these compounds stems from a very intense absorbance band at ~550 nm which has a molar extinction coefficient of 5800 M^{-1} cm^{-1} for (μ-NH,NH)[Fe^{III}(tbibt)(tbitbs•)]$_2$ and 14000 M^{-1} cm^{-1} for (μ-S,S)[Fe^{III}(tbibt)(tbitbs•)]$_2$ [26]. These are considered ligand-to-ligand intervalence charge transfer (LLIVCT) bands, underscoring the ligand-centered oxidation. The isomer shifts of 0.20 and 0.17 mm s^{-1}, and quadrupole splittings of 2.67 and 2.73 mm s^{-1} for the (μ-NH,NH) and (μ-S,S) isomer, respectively, indicate two intermediate-spin Fe(III) central ions; the smaller isomer shift upon ligand oxidation parallels the same trend described for the bis(dithiolene) systems. The temperature-dependent magnetic susceptibility measurements were modeled using two exchange coupled subspins of $S^* = 1$, where S^* stems from the antiferromagnetically coupled intermediate-spin Fe(III) ($S_{Fe} = 3/2$) with one ligand radical ($S_L = 1/2$). Although fictitious, it has physical meaning and a coupling constant of $J = -330$ cm^{-1} was computed.

Sellmann et al. prepared iron compounds with a tetradentate bis(aminobenzenethiolate) ligand, where the two halves are bridged by ethane [79]. The dialkali salt of this ligand is combined with hydrated ferrous chloride to produce what as formulated as [Fe(bmae)]$_x$, where $(bmae)^{2-}$ = 1,2-bis(2-mercaptoanilino)ethane (Scheme 4). Alternatively, the compound could be prepared via borohydride reduction of [Fe(gma)], where gma = glyoxal-bis(2-mercaptoanil) — a tetradentate bis(aminobenzenethiolate) bridged by an ethylene moiety [80], or thermal decarbonylation of [$Fe(CO)_2$(bmae)] [81]. The synthesis was repeated recently and its Mössbauer spectrum was recorded at 80 K [25]. The isomer shift and quadrupole splitting are similar to the bidentate aminobenzenethiolate complexes that indicate this compound consists of two high-spin ferrous ions with the tetradentate ligands in their dianionic form. The magnetic moment of 5.5 μ_B at 295 K underscores the dimeric nature of the complex and the temperature dependence over the temperature range of 4–300 K was modeled using two antiferromagnetic $S = 2$ spins with $J = -35$ cm^{-1} and $|D| = 10 \pm 5$ cm^{-1}.

A yellow precipitate of [Fe^{II}(bmae)]$_2$ handled in air quickly becomes black as the complex is oxidized according to Eq. (1):

$$[Fe^{II}(bmae)]_2 + O_2 \rightarrow [Fe^{III}(bmae^{\bullet})]_2 + 2H_2O \quad (1)$$

The redox level of the ligand is qualified by the X-ray structure analysis [26]. The unit cell contains three crystallographically independent dimers wherein the terminal N,S-coordinated half of the $(bmae)^{2-}$ ligand is an iminothionesemiquinonate radical as judged from their uniformly short C–S distances (avg. 1.728 Å) and the quinoid distortion of the corresponding six-membered rings. For the bridging part, the C–S distances are long (avg. 1.77 Å) and indicate the presence of an iminobenzenethiolate oxidation level, such that the tetradentate ligand is $(bmae^{\bullet})^{3-}$. This renders the central ion ferric and the complex is formulated [Fe^{III}(bmae•)]$_2$. Its Mössbauer spectrum consists of a 48:52 mixture of two quadrupole doublets: $\delta = 0.16$ mm s^{-1}, $\Delta E_Q = 2.68$ mm s^{-1}; $\delta = 0.25$ mm s^{-1}, $\Delta E_Q = 2.06$ mm s^{-1}, both consist of intermediate-spin ferric ($S_{Fe} = 3/2$) [26]. The diamagnetic ground state is a result of metal–metal and metal–ligand radical antiferromagnetic coupling. A consequence of the ligand oxidation sees a very intense LLIVCT band to appear in the electronic absorption spectrum.

4. Reactions of Fe-bis(dithiolene) and -bis(aminothiolate) complexes

Early research speculated that the dimeric dianions of the type $[Fe_2(L)_4]^{2-}$ existed as monomers, $[Fe(L)_2]^{1-}$, in solution [5,42,44,49,62,82]. It was soon realized that these monomers only came about when using polar, coordinating solvents such as pyridine (py), *N*,*N*′-dimethylformamide (dmf) and dimethylsulfoxide (dmso), otherwise in dichloromethane, tetrahydrofuran (thf) and acetone, the dimeric structure persisted. These solution studies were the first examples of dimer cleavage reactions to form five-coordinate adducts with the solvent. The following is a survey of the different types of small molecules that can cleave these iron bis(dithiolene) and bis(aminothiolate) dimers. Many of the products themselves form multi-membered electron transfer series, and we provide an overview of their varied molecular and electronic structures.

4.1. Lewis base adducts

4.1.1. Pyridines and amines

In 1966 [82], Gray et al. isolated the first stable five-coordinate adduct of an iron bis(dithiolene) during the preparation of $[Fe(tdt)_2]^{1-}$. Although the magnetic and spectroscopic properties of these complexes were altered by changing of the solvent from dichloromethane to dmf and dmso, these adducts were too labile to be isolated. However, when the reaction mixture containing the then formulated, [NBu_4][$Fe(tdt)_2$], was dissolved in pyridine, red plates of [NBu_4][$Fe(tdt)_2$·py] were isolated after addition of 2-propanol. Subjecting this compound to heat under high vacuum

for several hours purged the pyridine, leaving the purple microcrystalline $[NBu_4][Fe(tdt)_2]$ behind. The pyridine adduct has a room temperature magnetic moment of 3.94 μ_B that is consistent with a $S_t = 3/2$ ground state and electronic spectra very similar to the same Fe bis(dithiolene) anions in dmf or dmso.

McCleverty et al. [83,84] produced a surfeit of pyridine-based adducts with the different Fe bis(dithiolenes). Black crystalline compounds were isolated using an excess of a Lewis base, B = pyridine, α-, β-, γ-picoline, 4-aminopyrdine, 4-vinylpyridine, quinoline, isoquinoline, that in solution ranged from orange-brown ($[Fe(mnt)_2(B)]^{1-}$) to dark orange-red ($[Fe(tdt)_2(B)]^{1-}$). All were noted for having a quartet ground state and high lability in solution that precluded an electrochemical examination. Additionally, very stable, six-coordinate adducts were formed in the reaction of 2,2′-bipyridine (bpy) or *o*-phenanthroline (phen) with $[Fe_2(mnt)_4]^{2-}$ and $[Fe_2(tfd)_4]^{2-}$ [82–85]. These complexes will be discussed in Section 4.1.5. Dance and Miller isolated a plethora of $[Fe(mnt)_2(B)]^{1-}$ adducts, with the ammonia, *n*-butylamine, *tert*-butylamine, benzylamine, piperidine, morpholine, 3-azadicyclo[3.2.2]nonane, 4-cyanopyridine, 2-aminopyridine, imidazole, and 1-methylimidazole species [86]. They were characterized as having $S_t = 3/2$ ground states, and their formation constants were dictated by the basicity of the amine and its steric bulk. In solution they are in rapid reversible equilibrium between the five-coordinate adduct and the four-coordinate Fe bis(dithiolene) plus free base [85,86]. Adducts with ethylamine, triethylamine, tri-*n*-propylamine, aniline, and *p*-phenylenediamine did not yield isolable solids.

Eaton and Holm utilized this type of cleavage reaction to produce bridged binuclear bis(dithiolene) complexes of iron and cobalt [87]. The strategy involved adding an excess of various 4,4′-bipyridines in a high boiling point solvent that yielded complexes of the type $[Fe(L)_2–(B\text{-}B)–Fe(L)_2]^{0/2-}$ (L = $(mnt)^{2-}$, $(tfd)^{2-}$; B-B = bridging bipyridine); the complex charge was dependent on whether the dianionic or neutral bis(dithiolene) dimer was used. Two dinuclear complexes with bridging ethylenediamine and 1,4-diazacyclo[2.2.2]octane (dabco) were reported by Dance and Miller [86]. Like their mononuclear counterparts, these bridged binuclear species exhibited magnetic moments in the range of 3.98–4.17 μ_B indicating that no communication between planar $[Fe(L)_2]^{1-}$ units was affected by the bridging ligand [86,87].

A one-pot reaction of sodium metal, H_2tbbdt and 4-*tert*-butylpyridine (^{t}Bu-py) in ethanol was treated with $FeCl_3$ and $[PMePh_3]Br$ to give the dark red $[PMePh_3][Fe(tbbdt)_2(^t\text{Bu-py})]$ [14]. This compound was stable enough to obtain single crystals from a 1:1 dichloromethane/toluene solvent mixture at room temperature. From the crystal structure, shown in Fig. 13, it is clear that there are two closed-shell dianionic dithiolate ligands coordinated to an intermediate-spin Fe(III) ion ($S_{Fe} = 3/2$). Two other crystal structures of this type, namely $[NEt_4][Fe(etdt)_2(py)]$ ($etdt^{2-}$ = 1,2-diethyl-1,2-dithiolate) [88], and $[Fe(mnt)_2(idzm^+)]$ [57,89], where $(idzm)^+$ is the 2-(*p*-pyridyl)-4,4,5,5-tetramethylimidazolinium cation, show bond distances consistent with this electronic structure description. The latter is unique in that it is touted as having a $S_t = 3/2 \leftrightarrow S_t = 1/2$ spin-crossover at 1.5 K [89]. However, in view of the Mössbauer parameters posted in Table 4 [89,90], this phenomenon seems incompatible with an increase in the isomer shift for the minor species at temperature below 4.2 K such that it could be classified as a low-spin Fe(III) ($S_{Fe} = 1/2$) ion [91]. The same group was more successful in identifying spin-crossover in a rather curious compound, titled $[Fe(mnt)_2(rad^{\bullet+})]$, where $(rad^{\bullet})^+$ is the radical cation 2-(*p*-*N*-methylpyridinium)-4,4,5,5-tetramethylimidazoline-1-oxyl (Fig. 14) [90]. It was prepared from the reaction of $[Fe_2(mnt)_4]^{2-}$ and the $(rad^{\bullet+})I$; its crystal structure has metric parameters very similar to $[NBu_4][Fe(tfd)_2(OPPh_3)]$ [92]. The magnetic susceptibility data could only be accounted for by

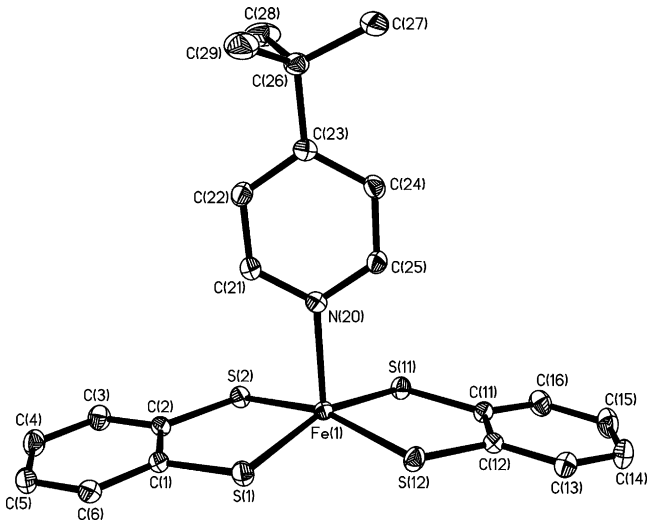

Fig. 13. Crystal structure of the monoanion in $PMePh_3[Fe(tbbdt)_2(^t\text{Bu-py})]$ [14].

Table 4
Experimental Mössbauer spectral parameters for iron bis(dithiolene) pyridine adducts.

Compound[a]	δ[b]	ΔE_Q[c]	S_{Fe}[d]	S_t[e]	Ref
$[Fe^{III}(mnt)_2(py)]^{1-}$	0.33	2.41	3/2	3/2	[69,70]
$[Fe^{III}(tfd)_2(py)]^{1-}$	0.33	2.61	3/2	3/2	[69]
$[Fe^{III}(Cl_4\text{-bdt})_2(py)]^{1-}$	0.33	3.02	3/2	3/2	[69]
$[Fe^{III}(tbbdt)_2(^t\text{Bu-py})]^{1-}$	0.33	3.03	3/2	3/2	[14]
$[Fe^{III}(tbbdt)(tbbdt^{\bullet})(^t\text{Bu-py})]^0$	0.29	3.02	3/2	1	[14]
$[Fe^{III}(qdt)_2(py)]^{1-}$	0.35	3.12	3/2	3/2	[71]
$[Fe^{III}(mnt)_2(\gamma\text{-pic})]^{1-}$[f]	0.36	2.59	3/2	3/2	[69]
$[Fe^{III}(mnt)_2(i\text{-quin})]^{1-}$[g]	0.36	2.46	3/2	3/2	[69]
$[Fe^{III}(mnt)_2(4\text{-}NH_2py)]^{1-}$	0.37	2.18	3/2	3/2	[69]
$[Fe^{III}(mnt)_2(idzm^+)]^0$[h]	0.33	2.48	3/2	3/2	[89]
	0.53	3.10	1/2	1/2	

[a] Ligand abbreviations available in Scheme 3.
[b] Isomer shift, mm s^{-1}.
[c] Quadrupole splitting, mm s^{-1}. The sign is unknown unless determined by an applied-field measurement.
[d] Intrinsic iron spin state.
[e] Total spin state of the complex.
[f] γ-pic = γ-picoline.
[g] *i*-quin = isoquinoline.
[h] Measured at 1.5 K. Parameters for the two subspectra are given.

a $S_t = 1$ spin ground state at temperatures exceeding 100 K that arises from the antiferromagnetic coupling of the intermediate-spin ferric ion ($S_{Fe} = 3/2$) with the unpaired spin on the ligand radical ($S_L = 1/2$). Below 100 K, a spin-crossover transition occurs where the singlet ground state is afforded by the antiferromag-

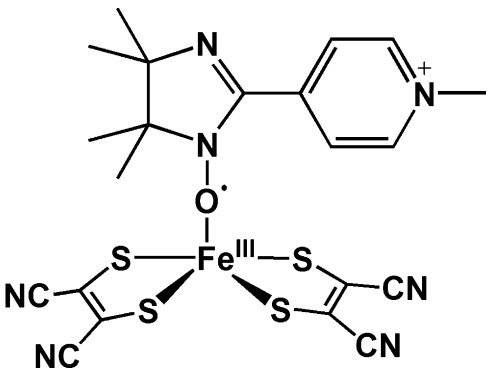

Fig. 14. Structure of $[Fe^{III}(mnt)_2(rad^{\bullet+})]$ [90].

netic coupling of a low-spin ferric center ($S_{Fe} = 1/2$) with the radical doublet spin.

Sellmann and co-workers have produced a raft of iron five- and six-coordinate mononuclear and dinuclear complexes with pentadentate NS_4 ligands [93], where two benzenedithiolates are bridged by a 2,6-dialkylpyridine moiety. An impressive array of exquisite reaction chemistry has been investigated with numerous small molecules such as phosphines, phosphites, carbon monoxide, nitric oxide, hydrazines, azide and solvents; their molecular and electronic structures, interconversion reactions and relevance to bioinorganic chemistry have been explored.

The stability of $[PMePh_3][Fe(tbbdt)_2(^tBu\text{-}py)]$ rendered it amenable to both electrochemical and chemical oxidation. Its cyclic voltammogram exhibited one reversible oxidation at −0.175 V (*vs.* Fc^+/Fc) and the controlled-potential coulometric generation of this neutral species was characterized by new intense absorption bands in the near-infrared region (>600 nm). The defining indicator that this redox process is ligand-centered comes from Mössbauer spectroscopy, in that both the isomer shift and quadrupole splitting remain almost stationary after the one-electron oxidation (Table 4). For $[Fe(tbbdt)_2(^tBu\text{-}py)]^{1-}$, the $\delta = 0.30\ mm\ s^{-1}$ and $\Delta E_Q = 3.03\ mm\ s^{-1}$ values define an intermediate-spin ferric ion; the same values are seen for monomeric $[Fe^{III}(qdt)_2]^{1-}$ in Section 2.1, and the dimeric bis(dithiolene) complexes described in Section 3.1.2. All known bis(dithiolene) pyridine adducts have the same electronic structure, with identical isomer shifts and large quadrupole splittings observed [14,69,83,89]. The quadrupole splittings are slightly smaller for the $(mnt)^{2-}$ and $(tfd)^{2-}$ compared to systems with aromatic dithiolates due to the former being stronger π acids. The instability of $[Fe(mnt)_2(4\text{-}NH_2py)]^{1-}$ has been attributed to the potential ability for the amine to bind another $[Fe(mnt)_2]^{1-}$ unit and generate a polymeric chain of six-coordinate monomers [84]. The higher coordination number is consistent with the lower quadrupole splitting of this species compared to its five-coordinate analogues [69].

The qualitative molecular orbital manifold shown in Fig. 15 for $[Fe^{III}(bdt)_2(py)]^{1-}$ shows one empty, one doubly occupied, and three singly occupied Fe d orbitals [94]. The Mulliken spin density analysis locates three unpaired electrons at the iron atom, with a small amount of spin density on the pyridine nitrogen due to covalency. One-electron oxidation of this monoanion generates a neutral species with the same 3d orbital occupancy plus an additional ligand-centered SOMO (Fig. 16). The orbital integral overlap value of S = 0.61 underscores the strong antiferromagnetic coupling between the metal and ligand radicals that affords the triplet ground state. The Mulliken spin density plot for $[Fe^{III}(bdt)(bdt^{\bullet})(py)]^0$ shows three α-spins at the metal and a single β-spin spread over both dithiolene ligands. The calculated Mössbauer parameters ($[Fe^{III}(bdt)_2(py)]^{1-}$: $\delta = 0.39\ mm\ s^{-1}$, $\Delta E_Q = 3.43\ mm\ s^{-1}$; $[Fe^{III}(bdt)(bdt^{\bullet})(py)]^0$: $\delta = 0.34\ mm\ s^{-1}$, $\Delta E_Q = 3.17\ mm\ s^{-1}$) based on these electronic structures are in excellent agreement with the experimental values [94].

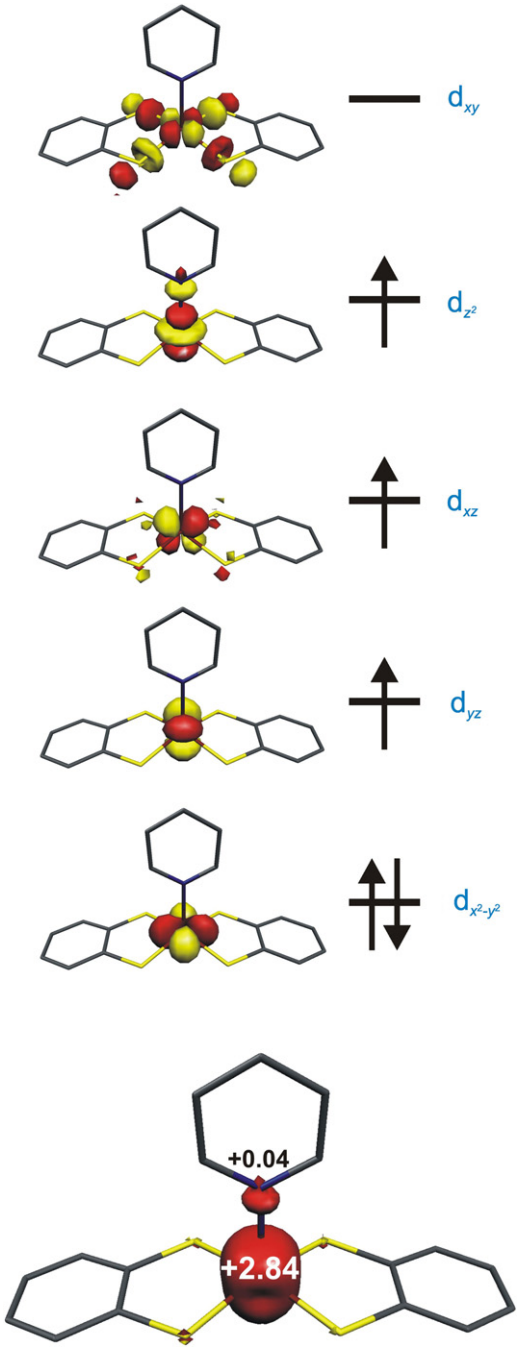

Fig. 15. Qualitative MO scheme for the $[Fe^{III}(bdt)_2(py)]^{1-}$ (top) and spin density plot together with a value of the spin density from a Mulliken spin population analysis (bottom) [94].

4.1.2. Phosphines, phosphites, arsines, and stibines

Schrauzer et al. demonstrated that the black insoluble residue from the reaction of $FeSO_4$ and $Na_2S_2C_2H_2$ afforded a soluble green crystalline compound when treated with tri-*n*-butylphosphine (P^nBu_3) [45]; it was formulated as $[Fe(S_2C_2H_2)_2{\cdot}P^nBu_3]$. Balch extended these reactions to arsines and stibines [95], though these were only performed with $[Fe_2(tfd)_4]$. The charge-neutral adducts are diamagnetic and polarography showed a reversible one-electron reduction to the monoanionic species $[Fe(tfd)_2{\cdot}(B)]^{1-}$ (B = Lewis base). These can be prepared by reacting the Lewis base with $[Fe_2(tfd)_4]^{2-}$ [83,84]. The second reduction was described as irreversible and associated with the loss of the Lewis base.

McCleverty synthesized a profusion of phosphine, phosphate, diphosphino, and arsine adducts using $(mnt)^{2-}$ [83,84,96], $(tfd)^{2-}$ [83,84,96], $(Cl_4\text{-}bdt)^{2-}$ [96], and a host of substituted $(pdt)^{2-}$ ligands [83,97]. The diphosphino ligand, (diphenylphosphino)ethane (dppe), was found to bind in a monodentate fashion, with the sole exception of $[NEt_4][Fe(mnt)_2(dppe)]$, which is suspected to be six-coordinate [96]. The tfd- and mnt-containing species with phosphines form a three-membered electron transfer series. The potential for the one-electron reduction responds to the basicity of the phosphine; the order of increasing negative potential being $P(CH_2CH_2CN)_3 < P(OPh)_3 < PEtPh_2 < P^iPr_3 < P(OEt)_3 < PEt_2Ph < PEt_3$ [84], the same order followed by the half-wave potentials for the $[PR_3]^{0/1-}$ couple [98]. For the pdt-containing systems, a

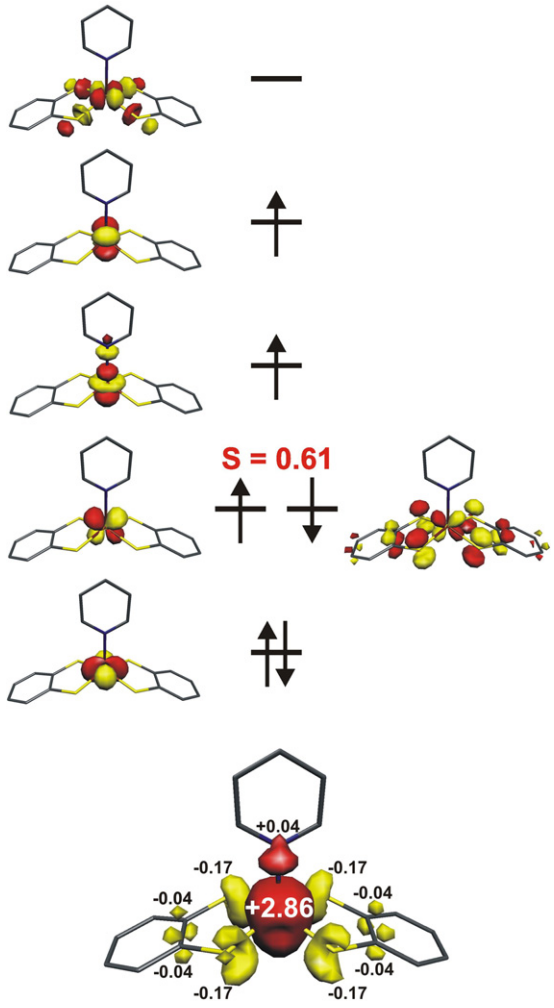

Fig. 16. Qualitative MO scheme for the $[Fe^{III}(bdt)(bdt^{\bullet})(py)]^{0}$ (top) and spin density plot together with a value of the spin density of the Mulliken spin population analysis (bottom) [94].

three-membered electron transfer series also exists, although a more complicated electrochemical response was seen with the reduction to the monoanion. The cyclic voltammogram was cured with the addition of phosphine and a very fast scan rate [91], such that it clearly indicated loss of the coordinated Lewis base. The reversibility of this reduction is highly dependent on the substituents of the dithiolene ligand, while the stability of the monocation was compromised when using $P(NMe_2)_3$ [97].

Eaton and Holm introduced bidentate bis(phosphino)ligands to $[Fe_2(mnt)_4]^{2-}$ and $[Fe_2(tfd)_4]^{2-/0}$ under an inert atmosphere to exclude the formation of phosphine oxides [87]. The resultant dinuclear complexes, $[Fe(L)_2–(B\text{-}B)–Fe(L)_2]^{z}$ ($z = 0$, $2-$) are bridged by (diphenylphosphino)benzene (dppb) and (diphenylphosphino)ethylene (dppet), represented by (B-B). Reactions involving (diphenylphosphino)acetylene (dppa) yielded a 1:1 stoichiometry, $[Fe_2(tfd)_2(dppa)]$, which maybe two *cis* octahedral doubly bridged units. The electrochemistry, magnetic properties and electronic absorption spectra were examined and communication across the bridging ligand was assessed [87].

The crystal structure of $[Fe(tfd)_2(AsPh_3)]$ first appeared briefly in 1970 [92], with the full crystal structure analysis not entering the literature until 1977 [99]. It has a square pyramidal Fe center displaced 0.23 Å out of the S_4 basal plane. The Fe–As bond distance of 2.325 Å and the $(tfd)^{2-}$ ligands have short C–S (av. 1.702 Å) and long C–C (av. 1.372 Å) bond lengths consistent with oxidized ligands. The

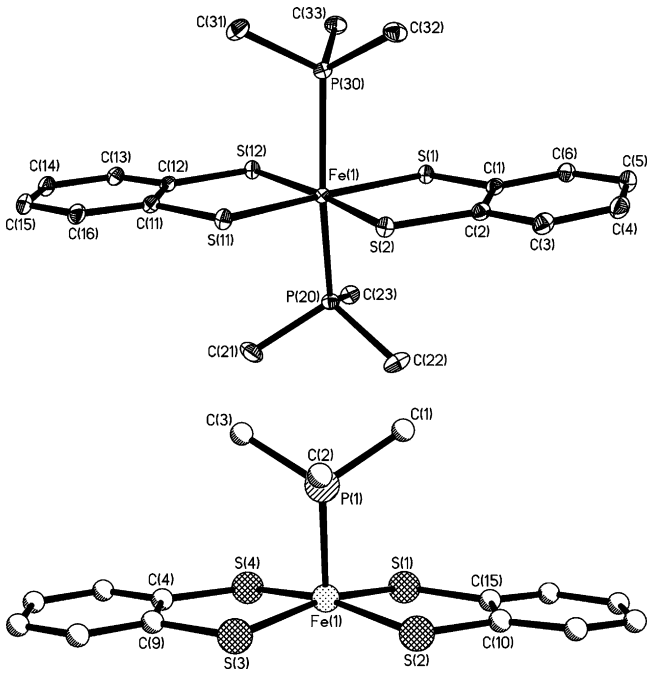

Fig. 17. Crystal structures of $[Fe(bdt)_2(PMe_3)_2]$ and $[Fe(bdt)_2(PMe_3)]$ [9,14].

monomeric units are orientated such that the Fe···S and Fe···Fe intermolecular distances are 4.178 and 4.788 Å, respectively. Dark green crystals of $Fe(pdt)_2\{P(OMe)_3\}$ was the first phosphite adduct to be characterized by X-ray crystallography [100]. Much like the arsine adduct, the Fe atom adopts a square pyramidal geometry, with the central ion 0.337 Å above the bis(dithiolene) equatorial plane. Again, short C–S and long C–C bonds point to oxidized dithiolene ligands. The Fe–P distance of 2.143 Å is, as expected, shorter than the arsine complex described above. Two other phosphine adduct structures derived from the cleavage an Fe bis(dithiolene) dimer have been reported [36,91]. On the whole, the Fe–P bond distance is ~2.14 Å for a phosphite and ~2.25 Å for a phosphine. Sellmann and co-workers prepared $[Fe(bdt)_2(PMe_3)_2]$ from a one-pot reaction of $FeCl_2{\cdot}4H_2O$, trimethylphosphine and $Na_2(bdt)$ (Fig. 17) [9]. This exists in equilibrium with $[Fe(bdt)_2(PMe_3)]$ (Fig. 17) in solution that can be manipulated by altering the amount of phosphine. Additionally, $[NMe_4][Fe(bdt)_2(PMe_3)_2]$ can be isolated via the same reaction with the inclusion of tetramethylammonium chloride under strictly anaerobic conditions [9]. $[Fe(bdt)_2(PMe_3)]$ can be chemically oxidized to the monocation [9]; this has been isolated with the $(tbbdt)^{2-}$ ligand [14]. Controversially, the original crystal structures of $[Fe(bdt)_2(PMe_3)_2]$ and $[Fe(bdt)_2(PMe_3)]$ were published as having a high-valent Fe(IV) with two closed-shell $(bdt)^{2-}$ ligands [9]. In both molecules, the dithiolene ligands have somewhat shorter average C–S bond distances (1.748 Å) than observed for $[Fe_2(bdt)_4]^{2-}$ (av. 1.763 Å). The six-coordinate $[Fe(bdt)_2(PMe_3)_2]$ has a distorted octahedral geometry: the Fe–P distances of 2.322 and 2.327 Å are significantly longer than the five-coordinate adducts, and the P–Fe–P angle is 159.8°. The Fe atom is perfectly planar with respect to the two dithiolene ligands and the Fe–S bond lengths average 2.241 Å. In contrast, the X-ray structural analysis of $[NEt_4][Fe(bdt)_2(PMe_3)_2]$ shows a very regular octahedral geometry with a P–Fe–P angle of 180°. The S–C bond distances are only slightly longer (av. 1.753 Å) than the neutral compound and the Fe–S bonds are also slightly longer at 2.253 Å. It is quite obvious that the resolution of the crystallography is insufficient to discern the oxidation level of the metal and the aromatic-1,2-dithiolate ligands.

Table 5
Experimental Mössbauer spectral parameters for iron bis(dithiolene) phosphine and phosphite adducts.

Compound[a]	δ[b]	ΔE_Q[c]	S_{Fe}[d]	S_t[e]	Ref
$[Fe^{III}(bdt)_2(PMe_3)_2]^{1-}$	0.29	1.67	1/2	1/2	[9]
$[Fe^{III}(tbbdt)_2(PMe_3)_2]^{1-}$	0.24	1.56	1/2	1/2	[14]
$[Fe^{III}(bdt^{\bullet})(bdt)(PMe_3)_2]^0$	0.17	1.54	3/2	1	[9]
$[Fe^{III}(tbbdt^{\bullet})(tbbdt)(PMe_3)_2]^0$	0.15	1.46	3/2	1	[14]
$[Fe^{III}(bdt^{\bullet})(bdt)(PMe_3)]^0$	0.12	3.03	3/2	1	[9]
$[Fe^{III}(tbbdt^{\bullet})(tbbdt)(PMe_3)]^0$	0.11	3.18	3/2	1	[14]
$[Fe^{III}(tbbdt^{\bullet})(tbbdt)(P^iPr_3)]^0$	0.09	3.19	3/2	1	[14]
$[Fe^{III}(tbbdt^{\bullet})_2(PMe_3)]^{1+}$	0.25	2.60	3/2	1/2	[14]
$[Fe^{II}(pdt^{\bullet})_2(PPh_3)]^0$	0.12	2.78	0	0	[69]
$[Fe^{II}(pdt^{\bullet})_2\{P(OPh)_3\}]^0$	0.08	2.55	0	0	[91]
$[Fe^{II}(pdt\text{-}p\text{-}^tBu^{\bullet})_2\{P(OMe)_3\}]^0$	0.06	−2.69	0	0	[91]
$[Fe^{III}(pdt^{\bullet})_2\{P(OPh)_3\}]^{1+}$	0.25	1.74	3/2	1/2	[91]
$[Fe^{II}(tbitbs^{\bullet})_2\{P(OPh)_3\}]^0$	0.06	2.92	0	0	[26]
$[Fe^{II}(bmae^{\bullet\bullet})_2(PPh_3)]^0$	0.04	3.16	0	0	[22]

[a] Ligand abbreviations available in Schemes 3 and 4.
[b] Isomer shift, mm s^{-1}.
[c] Quadrupole splitting, mm s^{-1}. The sign is unknown unless determined by an applied-field measurement.
[d] Intrinsic iron spin state.
[e] Total spin state of the complex.

Similar systems with aminobenzenethiolate ligands were provided by Sellmann et al., with a host of six-coordinate complexes generated in a one-pot reaction of $FeCl_2{\cdot}4H_2O$, Li_2bmaeH_2 and either PR_3 (R = Et, ^{n}Pr, ^{n}Bu), $P(OR')_3$ (R′ = Et, ^{n}Pr), (diphenylphosphino)methane (dppm), or dppe [81,101]. Several have been crystallized showing the phosphine/phosphite ligands in a *cis* conformation with a significant puckering of the ethane bridge of $(bmae)^{2-}$ [101]. It was further suggested that the $(bmae)^{2-}$ ligand stabilized high-valent Fe(IV) and Fe(V) [21,22]. The five-coordinate $[Fe(bmae)(P^nPr_3)]$ and $[Fe(bmae)(PPh_3)]$ complexes (formed in a one-pot reaction rather than cleavage of a dimer) are formally described as a Fe(IV) central ion bound by a $(bmae)^{4-}$ ligand in its tetraanionic form [22]. It is proposed that initially $[Fe^{II}(bmaeH_2)(PR_3)_2]$ is formed, and its subsequent exposure to air leads to deep blue-green $[Fe(bmae)(PR_3)]$ (R = Me, Et, ^{n}Pr, ^{n}Bu, Ph, Cy, OMe, OPh). However, the two crystal structures exhibit very short C–S and C–N bond lengths of ∼1.71 and ∼1.35 Å, respectively, that are incompatible with a closed-shell aminothiolate ligand. From these ligand dimensions, the PPh_3 and P^nPr_3 adducts were formulated as $[Fe^{II}(bmae^{\bullet\bullet})(PR_3)]$, where each aminobenzenethiolate arm is one-electron oxidized. Only $[Fe^{II}(tbitbs^{\bullet})_2\{P(OPh)_3\}]$ was prepared via a dimer cleavage reaction and its structural parameters are very similar to the $(bmae^{\bullet\bullet})^{2-}$ compounds [26].

An assignment of physical oxidation states for these phosphine adducts is offered by Mössbauer spectroscopy. The isomer shift and quadrupole splittings for the characterized complexes are displayed in Table 5 and show that a different iron oxidation state is assigned depending on whether the dithiolene ligand is olefinic, for example $(pdt)^{2-}$ [91], or aromatic, such as $(bdt)^{2-}$ [9,14]. This is

$$[Fe^{III}(L'^{\bullet})_2(PR_3)]^{1+} \underset{-e}{\overset{+e}{\rightleftharpoons}} [Fe^{II}(L'^{\bullet})_2(PR_3)]^0 \underset{-e}{\overset{+e}{\rightleftharpoons}} [Fe^{II}(L')(L'^{\bullet})(PR_3)]^{1-}$$
$$(S = {}^1/_2) \qquad (S = 0) \qquad (S = {}^1/_2)$$

Scheme 10. Ref. [91].

clearly evident from the crystallography, with two ligand radicals in the structure of $[Fe^{II}(pdt^{\bullet})_2\{P(OPh)_3\}]$ [91]. Since the compound is diamagnetic, the central ion must be low-spin Fe(II) ($S_{Fe} = 0$). Thus, the $\delta = 0.08$ mm s^{-1} and $\Delta E_Q = 2.55$ mm s^{-1} can be compared with its one-electron oxidized species, where the isomer shift changes markedly to $\delta = 0.25$ mm s^{-1} and quadrupole splitting decreases to $\Delta E_Q = 1.74$ mm s^{-1}. This paramagnetic $S_t = 1/2$ species possesses an axial EPR signal with ^{31}P hyperfine coupling and an electronic structure best described as $[Fe^{III}(pdt^{\bullet})_2\{P(OPh)_3\}]^{1+}$, where the ferric ion is intermediate-spin $S_{Fe} = 3/2$ [14,27]. Incidentally, coulometrically generated $[Fe(pdt)\{P(OMe)_3\}]^{1-}$ exhibits a nearly isotropic EPR signal with no resolved ^{31}P hyperfine that corresponds to a $[Fe^{II}(pdt)(pdt^{\bullet})\{P(OMe)_3\}]^{1-}$ electronic structure where the intrinsic spin state at Fe(II) is assumed to be $S_{Fe} = 1$; antiferromagnetic coupling of the ligand and metal produces the doublet ground state [91]. The magnitude of the ^{31}P hyperfine is consistent with the fluid solution measurements recorded by McCleverty et al. [84,97], though in the absence of Mössbauer data, a low-spin ferrous ion cannot be discounted. Interestingly, a room temperature magnetic moment of 3.97 μ_B was measured for $[Fe(tfd)_2(PPh_3)]^{1-}$ indicating a spin quartet ($S = 3/2$) [95]. It was subsequently shown that this was in fact a phosphine oxide complex, $[Fe(tfd)_2(OPPh_3)]^{1-}$ [92], due to aerial oxidation of triphenylphosphine. The electron transfer series is described in Scheme 10, where L′ is an olefinic dithiolene [91].

A combination of Mössbauer and EPR spectroscopy facilitated a reinterpretation of the redox behavior of $[Fe(tbbdt)_2(PMe)_x]$ ($x = 1$, 2) that does not included high-valent Fe(IV) (Scheme 11) [14]. Both complexes, in equilibrium in solution, have an intermediate-spin Fe(III) ($S_{Fe} = 3/2$), antiferromagnetically coupled to one ligand π radical ($S_L = 1/2$) to give a triplet ground state — $[Fe^{III}(bdt)(bdt^{\bullet})(PMe_3)_x]$ ($x = 1$, 2). Zero-field splittings of $D = -27$ cm^{-1} ($x = 1$) and $D = +16$ cm^{-1} ($x = 2$) are quintessentially intermediate-spin ferric. Moreover, the presence of C=S$^{\bullet}$ stretching frequencies and intense IVCT bands in the electronic absorption spectrum assist in classifying the ligand oxidation level to give a consistent electronic structure description for these molecules [15].

Recently, Donahue et al. exploited the loss of the phosphine upon electrochemical reduction of the adduct to develop a method of controlled phosphine binding [36]. Triphenylphosphine is introduced to $[Fe_2(pdt\text{-}p\text{-}OMe)_4]$ to produce the five-coordinate adduct. The application of a −1.0 V reducing potential liberates the phosphine and the monomeric bis(dithiolene) units dimerize. Switching the potential at the working electrode to +1.0 V regenerates the neutral dimer that sequesters phosphine to close the cycle (Scheme 12). Such a scheme can be applied to other Lewis bases, or mixtures, where the applied potential or the dithiolene ligand substituents can be used to modify the system for selective binding.

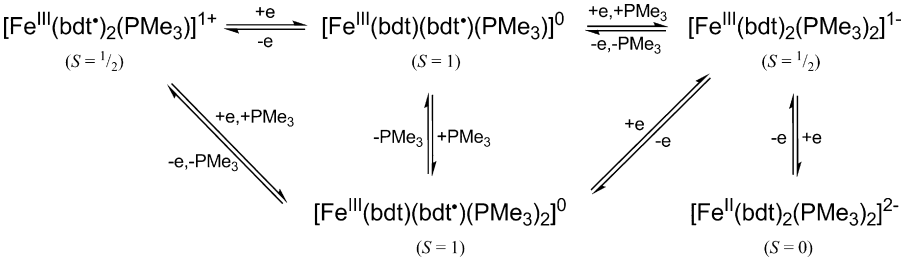

Scheme 11. Ref. [14].

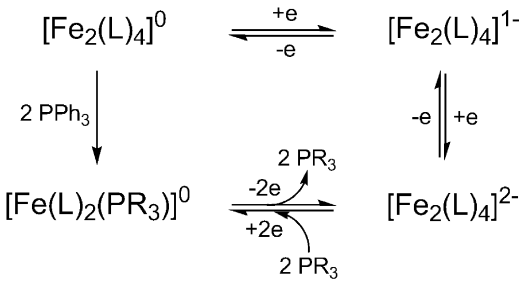

Scheme 12. Ref. [36].

4.1.3. Cyanide

McCleverty et al. cleaved both $[Fe_2(mnt)_2]^{2-}$ and $[Fe_2(tfd)_4]^{2-}$ with two equivalents of potassium cyanide and showed their room temperature magnetic moments are consistent with a $S_t = 1/2$ ground state [84]. Red-black $[NBu_4]_2[Fe(mnt)_2(CN)]$ and purple-brown $[PPh_4]_2[Fe(tfd)_2(CN)]$ exhibit similar electronic absorption spectra as the phosphine analogues that were quite different to Lewis base adducts of pyridines and nitric oxide. Other monoanionic nucleophiles such as azide and isocyanate also yielded five-coordinate adducts, while isothiocyanate and dicyanoamide proved unreactive [84]. In contrast to cyanide, these weak-field ligands produced quartet spin adducts similar to the pyridine systems. The cyanide adduct was revisited and the X-ray structure of dark green $[NBu_4][Fe(pdt\text{-}p\text{-}^tBu)_2(CN)]$ was solved [91]. The short C–S and long C–C bond distances clearly indicate a ferrous ion bound by two monoanionic π radical dithiolene ligands. The cyanide sits at a distance of 1.888 Å and the Fe atom floats 0.236 Å over the equatorial plane. $[NBu_4][Fe(pdt\text{-}p\text{-}^tBu)_2(CN)]$ forms a three-membered electron transfer series [91]; it can be reversibly one-electron oxidized and reduced. The cyanide stretching frequency responds primarily to the charge of the complex with the highest frequency ($2138\,cm^{-1}$) observed for the neutral species and the lowest frequency ($2047\,cm^{-1}$) for the dianionic complex. Moreover, each member exhibits a $\nu(C{=}S^{\bullet})$ stretch at $\sim 1154\,cm^{-1}$ and intense absorption bands >600 nm in their electronic spectra (Fig. 18). These are the hallmarks for dithiolene ligand radicals.

The intrinsic spin state of the central iron ion is derived from the Mössbauer spectral parameters. The mononanion has a small isomer shift of $0.11\,mm\,s^{-1}$ and negatively signed quadrupole splitting $\Delta E_Q = -2.55\,mm\,s^{-1}$ (from an applied-field measurement) are indicative of a low-spin Fe(II) ($S_{Fe} = 0$) ion, as seen for the phosphine and phosphite adducts. Reduction to $[Fe^{II}(L)(L^{\bullet})(CN)]^{2-}$ is ligand-centered with the ferrous ion now intermediate-spin ($S_{Fe} = 1$) antiferromagnetically coupled to one ligand radical ($S_L = 1/2$) to give a doublet ground state. The large isomer shift and quadrupole splitting are indicative of an intermediate-spin state, $S_{Fe} = 1$. The neutral complex, isolated from chemical oxidation of the monoanion by ferrocenium hexafluorophosphate, showed three quadrupole doublets in its Mössbauer spectrum. At 80 K, the spectrum was fitted in a 50:40:10 ratio that shifts to 58:30:12 at 4.2 K. At low temperatures, the dominant contribution comes from the quadrupole doublet described by $\delta = 0.26\,mm\,s^{-1}$ and $\Delta E_Q = 1.93\,mm\,s^{-1}$ that represents an intermediate-spin Fe(III) central ion. At room temperature, the ratio shifts to 30:70, with a dominant quadrupole doublet ($\delta = 0.65\,mm\,s^{-1}$, $\Delta E_Q = 0.65\,mm\,s^{-1}$) representative of a high-spin Fe(III) ($S_{Fe} = 5/2$). The temperature dependence of the ground state describes a $S_t = 3/2 \rightarrow 1/2$ gradual spin-crossover phenomenon. Similar behavior is witnessed for $Fe^{III}(L_{N,O}{}^{\bullet})Br$, where $L_{N,O}$ is the monoanionic π radical of the *o*-iminophenolate [102].

Density functional theoretical calculations on the monoanionic and neutral species augment the electronic structure elucidated from spectroscopy [91]. For $[Fe^{II}(L^{\bullet})_2(CN)]^{1-}$, three metal d orbitals are found to be doubly occupied, while the HOMO and the LUMO have 73% and 80% ligand character, respectively (Fig. 19). There are two empty d orbitals above the LUMO, such that overall, this orbital manifold confirms a low-spin ferrous ion coordinated by two monoanionic ligand π radicals. This scheme is contrasted by $[Fe^{III}(L^{\bullet})_2(CN)]$, where one doubly occupied and three singly occupied d orbitals define an intermediate-spin ferric center with two antiferromagnetic ligand π radicals (Fig. 20).

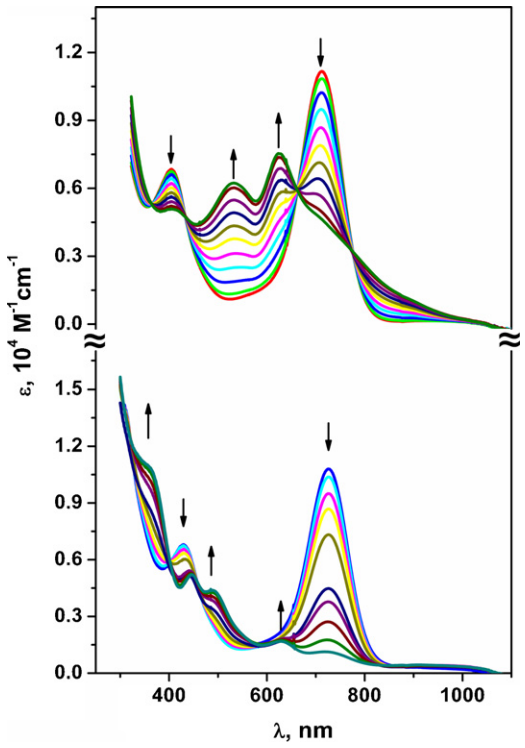

Fig. 18. Electronic spectral changes observed during the oxidation of $[Fe^{II}(pdt\text{-}p\text{-}^tBu^{\bullet})_2(CN)]^{1-}$ yielding $[Fe^{III}(pdt\text{-}p\text{-}^tBu^{\bullet})_2(CN)]^{0}$ (top), and reduction of $[Fe^{II}(pdt\text{-}p\text{-}^tBu^{\bullet})_2(CN)]^{1-}$ yielding $[Fe^{II}(pdt\text{-}p\text{-}^tBu)(pdt\text{-}p\text{-}^tBu^{\bullet})(CN)]^{2-}$ (bottom), in dichloromethane solution [91].

The spatial overlap of the α-spin (metal) and β-spin (ligand) SOMOs is strong ($S = 0.77$ and 0.57, respectively) and supports antiferromagnetic coupling to give the doublet ground state (Fig. 21). These electronic structures are validated by the computed Mössbauer parameters: $\delta = 0.16\,mm\,s^{-1}$, $\Delta E_Q = -2.62\,mm\,s^{-1}$ (exptl: $\delta = 0.11\,mm\,s^{-1}$, $\Delta E_Q = -2.55\,mm\,s^{-1}$) for $[Fe(pdt\text{-}p\text{-}^tBu)_2(CN)]^{1-}$ and $\delta = 0.17\,mm\,s^{-1}$, $\Delta E_Q = 2.05\,mm\,s^{-1}$ (exptl: $\delta = 0.25\,mm\,s^{-1}$, $\Delta E_Q = 1.93\,mm\,s^{-1}$) for $[Fe(pdt\text{-}p\text{-}^tBu)_2(CN)]$, which provide excellent agreement between experiment and theory [91,94].

4.1.4. Nitric oxide

Locke et al. communicated the first iron bis(dithiolene) dimer cleavage reaction with nitric oxide in 1966 [1], and described the $S_t = 1/2$ species $[Fe(L)_2(NO)]^{2-}$, where L represents either $(mnt)^{2-}$ or $(tfd)^{2-}$. The same compounds had been prepared *in situ* and their EPR spectra recorded [103], but it was not until they were isolated as solids that it was realized they formed a new series of mononitrosyl complexes related by one-electron transfer reactions [1]. McCleverty et al., in a spirit similar to their work with other Lewis bases, constructed extensive libraries of mononitrosyl complexes of iron with $(mnt)^{2-}$, $(tfd)^{2-}$, $(Cl_4\text{-}bdt)^{2-}$, $(tdt)^{2-}$ and various phenyl-substituted $(pdt)^{2-}$ dithiolene ligands [1,2,104]. It was shown that a three-member electron transfer series existed for $[Fe(mnt)_2(NO)]^z$, $[Fe(Cl_4\text{-}bdt)_2(NO)]^z$ ($z = 1-, 2-, 3-$), and $[Fe(tdt)_2(NO)]^z$ ($z = 0, 1-, 2-$), whereas $[Fe(tfd)_2(NO)]^z$ revealed four-members ($z = 0, 1-, 2-, 3-$) and $[Fe(pdt)_2(NO)]^z$ five-members ($z = +1, 0, 1-, 2-, 3-$). Isolation of two or more members of these electron transfer series

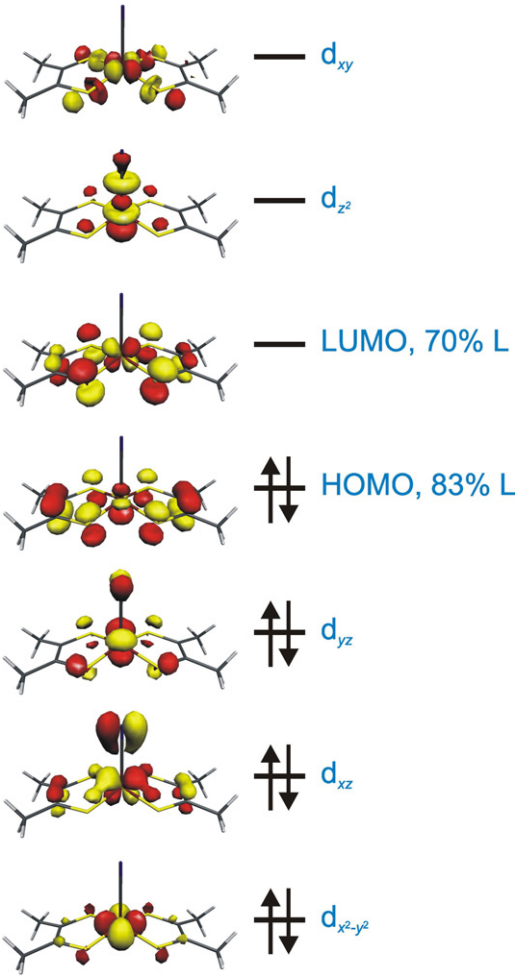

Fig. 19. Qualitative MO scheme for the $[Fe^{II}(L^{\bullet})_2(CN)]^{1-}$, where L = dithiolene [91].

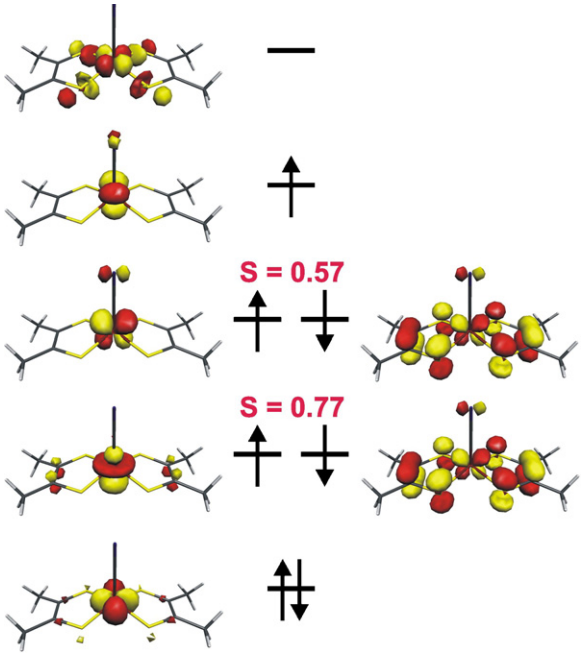

Fig. 20. Qualitative MO scheme for the $[Fe^{III}(L^{\bullet})_2(CN)]^{0}$ where L = dithiolene [91].

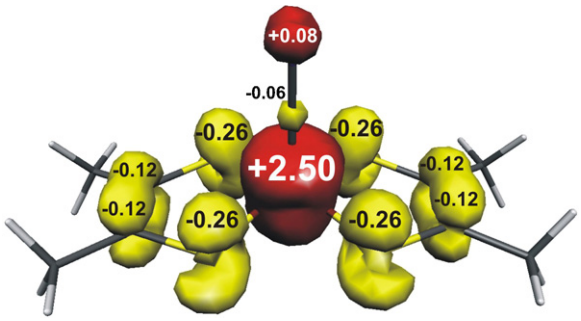

Fig. 21. Spin density plot and values from the Mulliken spin population analysis for $[Fe^{III}(L^{\bullet})_2(CN)]^{0}$ where L = dithiolene [91].

facilitated a comparison of the physical properties across a series and between different dithiolene ligands. The paramagnetic dianionic and neutral complexes, both $S_t = 1/2$, have strikingly different isotropic EPR spectra. Dianions are characterized by $g \sim 2.03$ with prominent hyperfine coupling of ~15 G from the ^{14}N nucleus ($I\{^{14}N\} = 1$) [1,2,104]. This hyperfine splitting is simplified with the introduction of ^{15}NO ($I\{^{15}N\} = 1/2$) [103]. The neutral complexes have $g \sim 2.009$ and no observed hyperfine splitting [1,2,104]. The ν(NO) stretching frequency varied 1650–1620 cm^{-1} for the dianions, 1870–1770 cm^{-1} for the monoanions, and just a narrow range of 1794–1802 cm^{-1} for the neutral complexes, though these all contained phenyl-substituted $(pdt)^{2-}$ dithiolenes. Around this time, the structure of $[Fe(mnt)_2(NO)]^{2-}$ was characterized by X-ray crystallography [105]. The intraligand distances of the $(mnt)^{2-}$ ligands proved to be consistent with their dianionic form, while the Fe–N–O angle is significantly bent at 168°. A correlation between the ν(NO) stretching frequency and the deviation of the oxygen atom away from the apical axis was thwarted by the large thermal motion of the oxygen atom that precluded an accurate measurement. The stretching frequency was dependent on the degree of π backbonding of the dithiolene ligand, which was modulated by the substituent [2]. Thus, complexes with $(mnt)^{2-}$ ligands have the highest stretching frequency; the order of increasing ν(NO) is $(mnt)^{2-} > (tfd)^{2-} > (Cl_4\text{-}bdt)^{2-} > (tdt)^{2-} > (pdt)^{2-}$. The same trend was observed for the redox potentials. Moreover, the large difference in the stretching frequency between the dianionic and monoanionic species of a particular series, compared with the relatively small, to nonexistent difference between monoanionic and neutral complexes, suggested a different electronic structure for the dianions on the one hand, with that of the monoanions and neutral species on the other.

The reaction of $[Fe_2(pdt)_4]$ with NO led to the formation of two products: one brown, the other purple [1,2,106]. The former is the monomeric compound, $[Fe(pdt)_2(NO)]$, whereas the latter was formulated as $[Fe_2(pdt)_2(NO)_2]$ [106]. It was quickly discovered that this composition was inaccurate, and that the dimeric species was in fact $[Fe_2(pdt)_3(NO)_2]$. This neutral dimeric compound also formed a three-membered electron transfer series as the cyclic voltammogram showed two reversible one-electron reductions to the monoanionic and dianionic forms [106].

The elucidation of the electronic structures of these iron nitrosyl complexes did not appear until very recently [107,108]. The complexity of these systems resides in its multiple redox active sites, that is (a) the NO ligand is the archetypal noninnocent ligand which can be bound to an iron ion as NO^+ ($S = 0$), NO ($S = 1/2$), or NO^- ($S = 0$ or 1), (b) the central ion can possess a d^6 ($S_{Fe} = 0$, 1, or 2) or d^5 ($S_{Fe} = 1/2$, 3/2, or 5/2) electron configuration, and (c) the dithiolene ligands may be coordinated as closed-shell dianion ($S_L = 0$) or as π radical monoanion ($S_L = 1/2$). Assigning a formal oxidation state to the iron ion is obviated by the introduction by Enemark and Feltham of the $\{FeNO\}^n$ notation where n corresponds to the familiar num-

ber of d electrons on the metal when the nitrosyl ligand is formally NO^+ [109]. However, X-ray crystallography has been used to define the oxidation level of the dithiolene ligand, and in concert with other spectroscopic measurements, a complete electronic assignment for the maximally five-membered electron transfer series was executed (Scheme 13).

There are two additional crystal structures of dianionic complexes, namely $[Fe(tdt)_2(NO)]^{2-}$ and $[Fe(Cl_2\text{-}bdt)_2(NO)]^{2-}$ [110], that possess intraligand bond distances consistent with two closed-shell aromatic dithiolate ligands. Moreover, the Fe–NO unit is bent (151.8° and 153.4°, respectively) and given the clear ^{14}N hyperfine coupling in the room temperature and frozen solution EPR spectra [107,111], this indicates coordinated a nitrosyl ($NO^\bullet$) radical ($S_L = 1/2$). Thus, the central ion is low-spin Fe(II) ($S_{Fe} = 0$). The Mössbauer spectra for these dianions have isomer shifts ranging 0.20–0.33 mm s^{-1} and, more importantly, small quadrupole splittings of 0.79–1.16 mm s^{-1} consistent with a diamagnetic ferrous ion.

Diamagnetic $[Fe(L)_2(NO)]^{1-}$ has been crystallographically characterized four times, where L = $(mnt)^{2-}$ [112], $(pdt\text{-}p\text{-}Me)^{2-}$ [107], $(Cl_2\text{-}bdt)^{2-}$ [110], and $(bdt)^{2-}$ [113]. Here, the C–S bond distances of 1.723, 1.746, 1.733 and 1.741 Å, respectively, are significantly shorter than the corresponding dianions described above that would suggest degree of dithiolene ligand oxidation. However, the most salient structural feature is the nearly linear Fe–NO unit: 180°, 176.2°, 177.6°, and 176.2°, respectively. Together with the pronounced increase in the ν(NO) stretching frequency of 170–205 cm^{-1}, this infers that the nitrosyl is now coordinated as NO^+ and that the monoanionic complexes are formulated as $[Fe^{II}(L)_2(NO^+)]^{1-}$, carrying a $\{FeNO\}^6$ core. The very small isomer shifts (δ = 0.01–0.05 mm s^{-1}) and reasonably large quadrupole splittings (ΔE_Q = 1.68–2.48) are not obviously attributable to low-spin Fe(II) ($S_{Fe} = 0$), however, strong π backbonding from the $(NO)^+$ removes electron density about the iron nucleus and creates a more anisotropic electron density distribution that generates these Mössbauer parameters [114].

The two neutral $Fe(L)_2(NO)$ complexes that have been analyzed by X-ray crystallography, where the dithiolene ligands are $(pdt\text{-}p\text{-}Me)^{2-}$ (Fig. 22) and $(pdt\text{-}p\text{-}Ph)^{2-}$ [107], as expected have very similar metric parameters. Both have short C–S bond distances of ~1.71 Å and long C–C bonds at ~1.39 Å that reveal oxidized dithiolene ligands with a linear Fe–NO unit. Most importantly, the change in the ν(NO) stretch when the monoanionic complex is oxidized is, on average, only 30 cm^{-1} [2,104,107], such that these neutral molecules are regarded as having an $\{FeNO\}^6$ core. Thus, the dithiolene ligand is oxidized and the frozen solution EPR spectrum is consistent with an unpaired electron on the dithiolene ligand given the small g-anisotropy and the absence of ^{14}N hyperfine coupling [107]. The electronic structure is defined as $[Fe^{II}(L)(L^\bullet)(NO^+)]$, and the Mössbauer parameters are very similar to those of the monoanionic complexes indicating again, a low-spin Fe(II) central ion. The only monocationic species to be chemically isolated is $[Fe(pdt\text{-}p\text{-}Me)_2(NO)](BF_4)$, obtained from the reaction of $[Fe_2(pdt\text{-}p\text{-}Me)_4]$ with $NOBF_4$ [107]. Like the monoanion and neutral species of this electron transfer series, the electronic spectrum of this monocation is dominated by intense absorption bands in the near-infrared region that are twice as intense as for the neutral compound. The shift in the ν(NO) frequency of only 33 cm^{-1} and given the similarity of the Mössbauer parameters (δ = 0.07 mm s^{-1}, ΔE_Q = 1.40 mm s^{-1}) [107], this compound is formulated as $[Fe^{II}(L^\bullet)_2(NO^+)]^+$, again with a $\{FeNO\}^6$ central core. The complete series is summarized in Scheme 13.

The crystal structures of neutral dinuclear $[Fe_2(pdt\text{-}p\text{-}Me)_3(NO)_2]$ (Fig. 22) and $[Fe_2(pdt\text{-}p\text{-}^tBu)_3(NO)_2]$ were very recently acquired [108]. Each square pyramidal, five-coordinate iron center is bound by four S atoms from two or three dithiolene

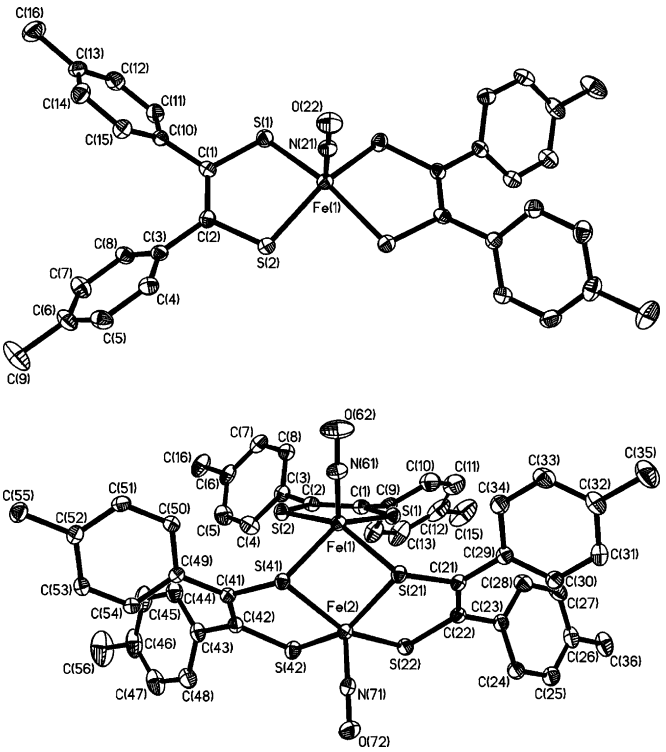

Fig. 22. Crystal structures of the neutral $[Fe(pdt\text{-}p\text{-}Me)_2(NO)]$ [107] and $[Fe_2(pdt\text{-}p\text{-}Ph)_3(NO)_2]$ [108].

ligands and one N atom from a nitrosyl ligand. From an assessment of the intraligand C–S and C–C bond distances, the terminal dithiolene ligand is a monoanionic π radical, while the two bridging dithiolene ligands are better described in their dianionic dithiolate

$$[Fe^{II}(NO)(pdt^\bullet)_2]^+ \quad S = 0$$

$$\text{-e} \rightleftharpoons \text{+e}$$

$$[Fe^{II}(NO)(pdt^\bullet)(pdt)]^0 \quad S = {}^1/_2$$

$$\text{-e} \rightleftharpoons \text{+e}$$

$$[Fe^{II}(NO)(pdt)_2]^{1-} \quad S = 0 \qquad \{FeNO\}^6$$

$$\text{-e} \rightleftharpoons \text{+e}$$

$$[Fe^{II}(NO^\bullet)(pdt)_2]^{2-} \quad S = {}^1/_2 \qquad \{FeNO\}^7$$

$$\text{-e} \rightleftharpoons \text{+e}$$

$$[Fe^{II}(NO)(pdt)_2]^{3-} \quad S = 0 \qquad \{FeNO\}^8$$

Scheme 13. Ref. [107].

$$\{[\{Fe^{II}(NO^{+})\}^{6}(L^{\bullet})]^{2+}[\{Fe^{II}(NO^{\bullet})\}^{7}(L)_2]^{2-}\}^{0}$$
$$S = 0$$
$$\text{-e} \rightleftharpoons \text{+e}$$
$$\{[\{Fe^{II}(NO^{\bullet})\}^{6}(L^{\bullet})]^{1+}[\{Fe^{II}(NO^{\bullet})\}^{7}(L)_2]^{2-}\}^{1-}$$
$$S = {}^{1}/_{2}$$
$$\text{-e} \rightleftharpoons \text{+e}$$
$$\{[\{Fe^{II}(NO^{\bullet})\}^{6}(L)]^{0}[\{Fe^{II}(NO^{\bullet})\}^{7}(L)_2]^{2-}\}^{2-}$$
$$S = 0$$

Scheme 14. Ref. [108].

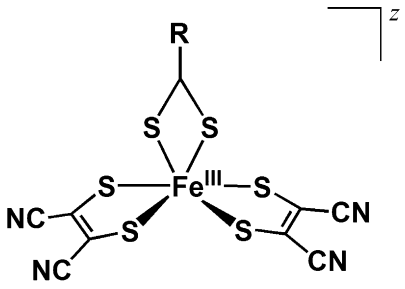

z = 2-, when R = $N(Me)_2$, $N(Et)_2$,
z = 3-, when R = $C(CN)_2$, N(CN), C(CN)($CONH_2$), C(CN)(CO_2Et), $CH(NO_2)$

Scheme 15.

form. To balance the charge, one center is $\{FeNO\}^7$ while the other is $\{FeNO\}^6$, which is certainly in keeping with the two ν(NO) stretches of 1754 and 1809 cm^{-1} for $[Fe_2(pdt\text{-}p\text{-}Me)_3(NO)_2]$, and 1768 and 1810 cm^{-1} for $[Fe_2(pdt\text{-}p\text{-}^tBu)_3(NO)_2]$ [108]. Each Mössbauer spectrum consists of two quadrupole doublets of equal intensity, with $\delta = 0.07$ mm s^{-1}, $\Delta E_Q = 1.57$ mm s^{-1} and $\delta = 0.22$ mm s^{-1}, $\Delta E_Q = 1.16$ mm s^{-1}, respectively, for $[Fe_2(pdt\text{-}p\text{-}Me)_3(NO)_2]$. The latter quadrupole doublet has similar parameters to the $\{FeNO\}^7$ unit in the mononuclear dianions (see above) whereas the former is archetypical of $\{FeNO\}^6$, with both iron centers in the +II oxidation state, and both low-spin ($S_{Fe1} = S_{Fe2} = 0$). Therefore, the diamagnetic ground state is derived from antiferromagnetic coupling between one NO• ($S = 1/2$) and a monoanionic π radical dithiolene ($S = 1/2$) mediated by the $[Fe_2S_2]$ central core. Chemical reduction of the neutral binuclear compound with cobaltocene generates a light green precipitate of $[CoCp_2][Fe_2(pdt\text{-}p\text{-}^tBu)_3(NO)_2]$ [108]. This salt is paramagnetic ($S_t = 1/2$) and displays a nearly isotropic frozen solution EPR spectrum devoid of any hyperfine features indicating the presence of a sulfur-centered radical. The electronic absorption spectrum has an intense band at 1200 nm and the shift in the ν(NO) stretches to 1734 and 1689 cm^{-1} shows the dithiolene radical has been retained with now two equivalent $\{FeNO\}^7$ units. Its Mössbauer spectrum exhibits a single quadrupole doublet with $\delta = 0.25$ mm s^{-1} and $\Delta E_Q = 0.96$ mm s^{-1}. The dianionic species shows no intense absorption bands in the region >800 nm and the ν(NO) stretch is very broad, but more or less unchanged at 1638 cm^{-1}. The electronic structures of these three members of this series are profiled in Scheme 14.

4.1.5. Bidentate Lewis bases

Strong donor ligands such as 2,2′-bipyridine and *o*-phenanthroline readily cleave iron bis(dithiolene) dimers to form, in contrast to their monodentate pyridine analogues, very stable six-coordinate complexes [82,84,85]. McCleverty et al. have prepared orange-brown $[Fe(mnt)_2(B\text{-}B)]^{1-}$ and blue-grey $[Fe(tfd)_2(B\text{-}B)]^{1-}$ with (B-B) = 2,2′-bipyridine (bpy) and *o*-phenanthroline (phen). These results were paralleled in a spectroscopic and kinetic study of these six-coordinate adducts with ethylenediamine, 2,2′-bipyridine and *o*-phenanthroline [85]. All these species are characterized by a room temperature magnetic moment of ~1.85 μ_B and fluid solution EPR spectra with g ~2.085. This signal was destroyed after addition of molecular iodine. At 77 K, an axial g-tensor was observed [85]. These compounds are reversibly one-electron oxidized and reduced, so presumably the iodine oxidizes to a neutral species with integer spin ($S = 0$ or 1). The Mössbauer spectra of $[Fe(mnt)_2(bpy)]^{1-}$ and $[Fe(mnt)_2(phen)]^{1-}$ at 80 K consist of a single quadrupole doublet with $\delta = 0.32$ mm s^{-1}, $\Delta E_Q = 1.85$ mm s^{-1}, and $\delta = 0.31$ mm s^{-1}, $\Delta E_Q = 1.80$ mm s^{-1}, respectively [69]. These values are used to assign a $[Fe^{III}(L)_2(B\text{-}B)]^{1-}$ electronic structure, with a central low-spin iron ($S_{Fe} = 1/2$) ion. McCleverty and Orchard prepared an analogous six-coordinate diphosphino complex, $[NEt_4][Fe(mnt)_2(dppe)]$ [96], whose electronic absorption spectrum closely resembles that for the bidentate N-donor complexes. It was therefore concluded that this species is probably six-coordinate, rather than bridging two planar iron bis(dithiolene) units [87], or a five-coordinate adduct with the dppe bound in a monodentate fashion [96]. This species was oxidized to the neutral form, though it is unclear whether this is five- or six-coordinate.

Bidentate sulfur-donor ligands such as dithiocarbamates, $(dtc)^{1-}$, and 1,1-dithiolates can be added to $[Fe_2(mnt)_4]^{2-}$ to produce a monomeric complex with an FeS_6 polyhedron [115,116]. McCleverty and co-workers prepared a series of such complexes, as outlined in Scheme 15, where each contained a low-spin ferric ion ($S_{Fe} = 1/2$). Additionally, it was also shown that dialkali salts of 1,2-dithiolene ligands are capable of cleaving the bis(dithiolene) dimer to form tris(dithiolene) complexes. These have been reported for $[Fe(mnt)_3]^{3-}$ [85], $[Fe(mnt)_3]^{2-}$ [117], and $[Fe(Cl_4\text{-}bdt)_3]^{2-}$ [118]. For the latter, the first product was not a trianion as is the case for the mnt species. Both $[Fe^{III}(mnt)_3]^{3-}$ and $[Fe^{III}(mnt)_2(Etdtc)]^{2-}$ ($Etdtc^{1-}$ = diethyldithiocarbamate) have been structurally characterized [116]; each contain a distorted octahedral FeS_6 core. Both compounds contain low-spin Fe(III) ions that are coordinated by three closed-shell dithiolate or dithiocarbamate ligands. Their Mössbauer isomer shifts ($\delta = 0.39$ and 0.36 mm s^{-1}, respectively) and quadrupole splittings ($\Delta E_Q = 1.77$ and 1.68 mm s^{-1}, respectively) [69,70,116,119] are the similar to the bidentate nitrogen-donor adducts. However, they have room temperature magnetic moments ranging 2.50–2.60 μ_B [115], and although these are significantly higher than the bidentate N-donor adducts, they are similar to the values for the spin doublet tris(dithiolene) complexes [117,120]. The rhombic EPR spectrum ($g = 2.14, 2.10, 2.01$) for $[Fe(mnt)_3]^{3-}$ could only be obtained at liquid helium temperatures [121], in contrast to the N- and P-donor analogues.

One-electron oxidation of these six-coordinate complexes is very facile; for $[Fe(mnt)_3]^{3-}$ it occurs on the bench in air [85]. Each of the FeS_6 compounds in Scheme 15 exhibit either reversible or quasi-reversible one-electron oxidations; the Mössbauer parameters would suggest that this is metal-centered [69,70,116,122]. There is certainly a slight shortening of the Fe–S bond lengths to assign the oxidized products as Fe(IV) ($S = 1$) compounds [116,123], though it must be noted that the highly covalent Fe–S bonds renders such an oxidation state assignment somewhat ambiguous and that no comparisons can be made with the ferryl $[Fe^{IV}O]^{2+}$ entity. Only four compounds have been isolated, namely $[Fe(mnt)_3]^{2-}$ [117], $[Fe(Cl_4\text{-}bdt)_3]^{2-}$ [118], $[Fe(mnt)_2(Etdtc)]^{1-}$ [116], and $[Fe(mnt)_2\{S_2C{:}C(CN)_2\}]^{1-}$ [115]; each have magnetic moments close to 2.8 μ_B for $S_t = 1$ species. It is not known whether

the N- and P-containing adducts also stabilize a reputed Fe(IV), but it seems highly plausible by analogy to systems with three bidentate sulfur-donor ligands. It would appear that six-coordinate adducts, formed by three bidentate ligands manage to coordinate to a high-valent iron ion that is not seen for other adducts.

Yandell and Sutin treated $[Fe(mnt)_3]^{2-}$ with a selection of inorganic bases that reacted according to Eq. (2) (B = PPh_3, $OPPh_3$, $AsPh_3$, $OAsPh_3$, py), which were monitored by UV–visible spectroscopic measurements [85]. The same bases did not react with the corresponding tris(dithiolene) trianion:

$$2[Fe(mnt)_3]^{2-} + 2B \rightarrow 2[Fe(mnt)_2(B)]^{1-} + [(mnt)_2]^{2-} \quad (2)$$

As described previously, the formed adducts had a $S_t = 3/2$ ground state, with the sole exception of $[Fe^{III}(mnt)_2(PPh_3)]^{1-}$, which as noted previously (Section 4.1.2), has a $S_t = 1/2$ ground state.

4.2. Halogens

In reactions with dimeric bis(dithiolene) and bis(aminothiolate) complexes, halogens, in particular iodine, are employed as oxidizing agents. However, it seems that the resultant halide ions are able to cleave the weakened Fe–S bonds to form neutral five-coordinate complexes. There are two examples of bis(dithiolene) complexes, namely [Fe(etdt)$_2$I] [88], and [Fe(pdt-*p*-^{t}Bu)$_2$I] [91] that were formed via oxidation of the parent $[Fe_2(L)_4]$ with molecular iodine. Initially, $[Fe_2(etdt)_4]^{2-}$ was prepared under anaerobic conditions [88], and this was treated with three equivalents of iodine, whereas [Fe(pdt-*p*-^{t}Bu)$_2$I] was retrieved from the mixture of equimolar amounts of $[Fe_2(pdt\text{-}p\text{-}^tBu)_4]$ and I_2 [91]. It would seem likely that first iodine oxidizes $[Fe_2(etdt)_4]^{2-}$ to the neutral dimer, and further oxidation, in this instance of a bridging ligand, weakens the Fe–S bond to the extent that it is readily supplanted by iodide. The X-ray structural analysis of [Fe(etdt)$_2$I] shows very short C–S bond distances (avg. 1.699 Å) and long C–C distances (avg. 1.382 Å) unambiguously confirm two monoanionic π radical dithiolene ligands [88], such that the reaction is described by Eq. (3), where the two dianionic bridging dithiolene ligands have been one-electron oxidized.

$$[Fe^{III}{}_2(L)_2(L^{\bullet})_2]^0 + I_2 \rightarrow 2[Fe^{III}(L^{\bullet})_2I]^0 \quad (3)$$

These complexes have a doublet spin ground state, and EPR spectra consistent with an iron-centered paramagnet [91]. The $S_t = 1/2$ arises from strong antiferromagnetic coupling between the two dithiolene radicals ($S_L = 1$) and an intermediate-spin Fe(III) ($S_{Fe} = 3/2$) central ion. The most unique feature of these systems appears in their X-band EPR spectra that display a complicated line pattern centered on g_{min} ascribed to iodine ($I\{^{127}I\} = 5/2$, 100% natural abundance) hyperfine coupling (Fig. 23) [91]. The spectrum could only be simulated with the inclusion of a large electric quadrupole interaction from the halide that is rotated 'off' the principle axes of the corresponding magnetic hyperfine. The major components of the electric field gradient tensor are found along g_{max} which is perpendicular to A_{max}, centered on g_{min}. This phenomenon is inherent to the EPR spectra of all halide adducts regardless of the nature of the two ligand π radicals [26,102,124]. The electronic structure is very similar to $[Fe^{III}(L^{\bullet})_2(CN)]^0$ (Section 4.1.3), with the Mulliken spin population analysis showing three unpaired electrons on the ferric ion (intermediate-spin, $S_{Fe} = 3/2$) and two unpaired electrons dispersed over the dithiolene ligands.

The somewhat controversial assignment of an Fe(V) ion in [Fe(bmae)I] required the $(bmae)^{4-}$ ligand to be in its fully reduced, closed-shell form [21]. This description is incompatible with the short C–S and C–N bond distances at 1.719 and 1.342 Å, respectively, which are not indicative of single bonds. From this structure, the compound was re-formulated as $[Fe^{III}(bmae^{\bullet\bullet})I]$

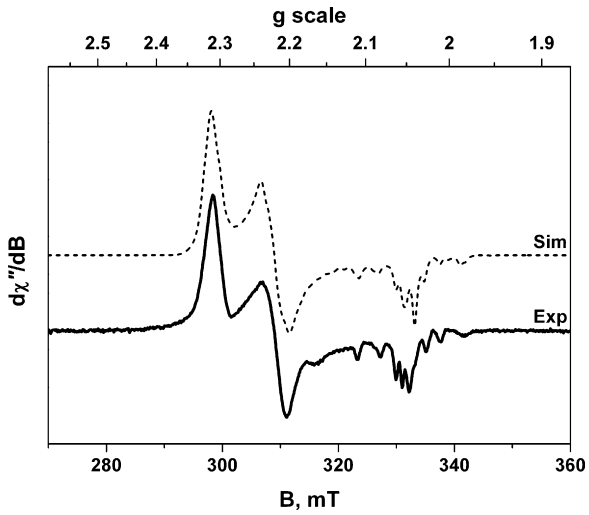

Fig. 23. X-band EPR experimental spectrum and simulation for [Fe(pdt-*p*-^{t}Bu)$_2$I] [91].

[26], where each aminobenzenethiolate arm of the tetradentate ligand has been one-electron oxidized. This is the only aminothiolate halide adduct to be crystallographically characterized [21], however, the series of $[Fe^{III}(tbitbs^{\bullet})_2X]$ (X = Cl, Br, I) and $[Fe^{III}(tbfitbs^{\bullet})_2I]$ have near-identical absorption bands at 560–540 nm with intensities exceeding $10^4\ M^{-1}\ cm^{-1}$ [26,39]. Fig. 24 shows the distinctive absorption band for these complexes that maybe described as a ligand-to-ligand charge transfer (LLCT) transition. The $[Fe^{III}(tbitbs^{\bullet})_2X]$ compounds were prepared via halogen oxidation of the dimeric $(\mu\text{-}S,S)[Fe^{III}(tbibt)(tbitbs^{\bullet})]_2$, where oxidation of a bridging $(tbibt)^{2-}$ ligand weakens the interlayer Fe–S bond that is subsequently cleaved by the halide [26]. The same products are obtained if $(\mu\text{-}NH,NH)[Fe^{III}(tbibt)(tbitbs^{\bullet})]_2$ is used. Sellmann and co-workers generated $[Fe^{III}(bmae^{\bullet\bullet})I]$ through I_2 oxidation of $[Fe^{II}(bmae^{\bullet\bullet})(P^nPr_3)]$ [21], whereas molecular iodine was added to monomeric $[Fe^{III}(tbfibt)_2]^{1-}$ to achieve the charge-neutral five-coordinate species [39]. Similar EPR spectra have been recorded for these doublet spin species, with the simulation requiring rotation of the electric quadrupole tensor for the iodo and bromo compounds [26]. No resolved hyperfine splittings were evident in the spectrum of $[Fe^{III}(tbitbs^{\bullet})_2Cl]$ [26]. This consistent picture of the electronic structure of these compounds is underscored by the narrow range of isomer shifts ($\delta = 0.11$–$0.21\ mm\ s^{-1}$) and quadrupole splittings ($\Delta E_Q = 2.63$–$3.41\ mm\ s^{-1}$) [21,26,39]

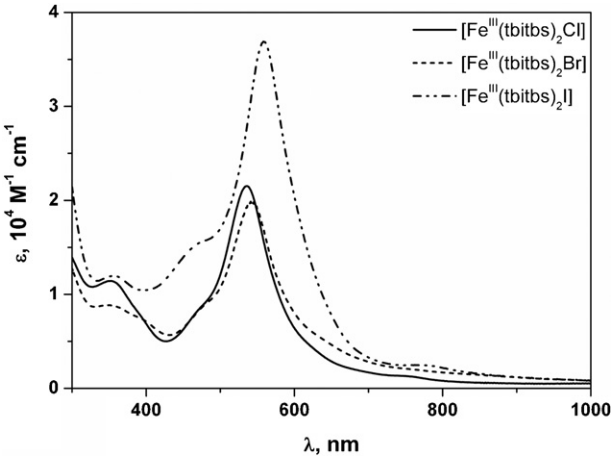

Fig. 24. Electronic absorption spectra for $[Fe^{III}(tbitbs^{\bullet})_2X]$, where X = Cl, Br, I [26].

that, much like previous discussions on the dimeric and five-coordinate adducts, identify an intermediate-spin central ion.

5. Summary

There is an immense variety of coordination complexes incorporating iron bis(dithiolene) and bis(aminothiolate) units; their physical and spectroscopic properties have been elucidated by crystallographic, spectroscopic and theoretical techniques. In essence, they can be categorized into nine groups, distinguished by their iron and ligand(s) oxidation levels. Many conclusions can be taken from the data summarized in Table 6, namely, and in no particular order: (1) the four-member electron transfer series for the dimeric iron bis(dithiolenes) are connected by ligand-centered redox processes, (2) the square-planer iron bis(dithiolene) and bis(aminothiolate), as well as their pyridine adducts, are benchmark examples for intermediate-spin ferric, (3) all nitrosyl-containing complexes contain low-spin ferrous ions, (4) the ligand and iron oxidation states in phosphine adducts is dependent on the type of dithiolene ligand (olefinic or aromatic), (5) strong-field ligands like cyanide or phosphine do not necessarily have a preference for low-spin iron states, when they displace a weak-field ligand such as pyridine, and (6) high-valent iron is not stabilized by dithiolene or aminothiolate ligands, with the possible, albeit ambiguous exception of iron ligated by three bidentate ligands.

Success in assigning a physical or spectroscopic oxidation state for the metal and ligands principally stems from X-ray crystallography and Mössbauer spectroscopy. For the former, the intraligand bond distances are the most useful measure of the ligand oxidation state, although there are several examples where this is not the case. Hence, it is important to look for signs of radical or oxidized ligands with spectroscopy, and these have been revealed in vibrational, optical, X-ray absorption, and magnetic resonance spectra of these systems. The effectiveness of Mössbauer spectroscopy is greatly enhanced when spectra of several members of a particular class of compound and several members of an electron transfer series are recorded, such that a self-consistent picture of their intrinsic electronic structure can be drawn. Gratifyingly, contemporary theoretical methods are up to the challenge, and efficiently reproduce the correct electronic structure that is readily calibrated and validated by calculation of spectroscopic observables, such as key vibrational frequencies and Mössbauer parameters.

The most prominent theme throughout this article is the fact that dithiolene and aminothiolate ligands, akin to their diimine, aminophenolate, dioxolene analogues, are clearly redox noninnocent. This message, heavily represented in our own chemistry, is one that we find needs to be continually raised in coordination chemistry. These compounds are classic examples where the chemistry and electronic structure is defined by the intrinsic redox interplay that exists between a redox active transition metal and a noninnocent ligand.

Table 6
Classification and overview of spin states adopted by monomeric and dimeric homoleptic iron bis(dithiolene) and bis(aminothiolate) complexes and their five- and six-coordinate adducts.

Type	Compound	S_{Fe}[a]	S_L[b]	S_t[c]
I	$[Fe^{III}{}_2(L)(L^{\bullet})_3]^{1+}$	3/2	3/2	1/2
II	$[Fe^{III}{}_2(L)_2(L^{\bullet})_2]^0$	3/2	1	0
	$[Fe^{III}(L^{\bullet})_2(CN)]^0$	3/2	1	1/2
	$[Fe^{III}{}_2(ibt)_2(itbs^{\bullet})_2]^0$	3/2	1	0
	$[Fe^{III}(L^{\bullet})_2(PR_3)]^{1+}$	3/2	1	1/2
	$[Fe^{III}(L^{\bullet})_2(X)]^0$	3/2	1	1/2
III	$[Fe^{II}(L^{\bullet})_2(CN)]^{1-}$	0	0	0
	$[Fe^{II}(L^{\bullet})_2(PR_3)]^0$[d]	0	0	0
	$[Fe^{II}(L^{\bullet})_2(NO^+)]^{1+}$	0	0	0
IV	$[Fe^{III}{}_2(L)_3(L^{\bullet})]^{1-}$	3/2	1/2	1/2
	$[Fe^{III}(L)(L^{\bullet})(py)]^0$	3/2	1/2	1
	$[Fe^{III}(mnt)(rad^{\bullet+})]^0$	3/2	1/2	1
		1/2	1/2	0
	$[Fe^{III}(bdt)(bdt^{\bullet})(PR_3)_x]^{1+}$	3/2	1/2	1
V	$[Fe^{II}(L)(L^{\bullet})(CN)]^{2-}$	1	1/2	1/2
	$[Fe^{II}(L)_2(NO^{\bullet})]^{2-}$	0	1/2	1/2
	$[Fe^{II}(L')(L'^{\bullet})(PR_3)]^{1-}$[e]	1	1/2	1/2
	$[Fe^{II}(L)(L^{\bullet})(NO^+)]^0$	0	1/2	1/2
VI	$[Fe^{III}{}_2(L)_4]^{2-}$	3/2	0	3/2
	$[Fe^{III}(L)_2]^{1-}$	3/2	0	0
	$[Fe^{III}(L)_2(py)]^{1-}$	3/2	0	3/2
	$[Fe^{III}(bdt)_2(PR_3)_2]^{1-}$	3/2	0	3/2
	$[Fe^{III}(tfd)_2(OPPh_3)]^{1-}$	3/2	0	3/2
	$[Fe^{III}(mnt)_2(idzm^+)]^0$	3/2	0	3/2
	$[Fe^{III}{}_2(ibt)_2(abt)_2]^0$	3/2	0	0
VII	$[Fe^{II}(L)_2(NO^-)]^{3-}$	0	0	0
	$[Fe^{II}(dtsq)_2]^{2-}$	2	0	2
	$[Fe^{II}(bdt)_2]^{2-}$	1	0	1
	$[Fe^{II}(L)_2(NO^+)]^{1-}$	0	0	0
	$[Fe^{II}{}_2(abt)_4]^0$	2	0	0
VIII	$[Fe^{III}(L)_2(S\text{-}S)]^{3-}$[f]	1/2	1/2	0
	$[Fe^{III}(L)_2(dtc)]^{2-}$[g]	1/2	1/2	0
	$[Fe^{III}(L)_2(N\text{-}N)]^{1-}$	1/2	1/2	0
	$[Fe^{III}(L)_2(dppe)]^{1-}$	1/2	1/2	0
XI	$[Fe^{IV}(L)_2(dtc)]^{2-}$	1	0	1
	$[Fe^{IV}(mnt)_3]^{2-}$	1	0	1

[a] Intrinsic spin state of the iron ion.
[b] Total spin of ligand(s).
[c] Total spin ground state of the complex.
[d] Not including aromatic dithiolenes.
[e] L′ = olefinic dithiolene.
[f] S-S = 1,1-dithiolate(2-) or 1,2-dithiolate(2-).
[g] dtc = dialkyldithiocarbamate(1-).

Acknowledgments

We greatly appreciate the assistance of Dr Thomas Weyhermüller in preparing all the crystal structure figures. We gratefully acknowledge financial support from the Fonds der Chemichen Industrie and S.S. thanks Max Planck Society for a postdoctoral fellowship.

References

[1] J. Locke, J.A. McCleverty, E.J. Wharton, C.J. Winscom, Chem. Commun. (1966) 677.
[2] J.A. McCleverty, N.M. Atherton, J. Locke, E.J. Wharton, C.J. Winscom, J. Am. Chem. Soc. 89 (1967) 6082.
[3] J.A. McCleverty, Prog. Inorg. Chem. 10 (1968) 49.
[4] A.L. Balch, I.G. Dance, R.H. Holm, J. Am. Chem. Soc. 90 (1968) 1139.
[5] H.B. Gray, E. Billig, J. Am. Chem. Soc. 85 (1963) 2019.
[6] An olefinic dithiolene with a bonafide C–C double bond is also described as a *true* dithiolene, while aromatic dithiolates, where the C–C bond is not localized, is termed a *pseudo* dithiolene. To our knowledge, there has been no identification of the fully oxidized form of an aromatic dithiolate, ie. a dithioquinone.
[7] (a) C.G. Pierpont, R.M. Buchanan, Coord. Chem. Rev. 38 (1981) 45; (b) C.G. Pierpont, C.W. Lange, Prog. Inorg. Chem. 41 (1994) 331.
[8] D. Sellmann, H. Binder, D. Häußinger, F.W. Heinemann, J. Sutter, Inorg. Chim. Acta 300–302 (2000) 829.
[9] D. Sellmann, M. Geck, F. Knoch, G. Ritter, J. Dengler, J. Am. Chem. Soc. 113 (1991) 3819.
[10] S. Bhattacharya, P. Gupta, F. Basuli, C.G. Pierpont, Inorg. Chem. 41 (2002) 5810.
[11] C. Milsmann, E. Bothe, E. Bill, T. Weyhermüller, K. Wieghardt, Inorg. Chem. 48 (2009) 6211.
[12] (a) P. Banerjee, S. Sproules, T. Weyhermüller, S. DeBeer George, K. Wieghardt, Inorg. Chem. 48 (2009) 5829; (b) R.R. Kapre, E. Bothe, T. Weyhermüller, S. DeBeer George, N. Muresan, K. Wieghardt, Inorg. Chem. 46 (2007) 7827; (c) C. Milsmann, G.K. Patra, E. Bill, T. Weyhermüller, S. DeBeer George, K. Wieghardt, Inorg. Chem. 48 (2009) 7430;

(d) K. Ray, S. DeBeer George, E.I. Solomon, K. Wieghardt, F. Neese, Chem. Eur. J. 13 (2007) 2783;
(e) K. Ray, T. Weyhermüller, A. Goossens, M.W. Crajé, K. Wieghardt, Inorg. Chem. 42 (2003) 4082;
(f) K. Ray, T. Weyhermüller, F. Neese, K. Wieghardt, Inorg. Chem. 44 (2005) 5345.
[13] T. Petrenko, K. Ray, K. Wieghardt, F. Neese, J. Am. Chem. Soc. 128 (2006) 4422.
[14] K. Ray, E. Bill, T. Weyhermüller, K. Wieghardt, J. Am. Chem. Soc. 127 (2005) 5641.
[15] K. Ray, T. Petrenko, K. Wieghardt, F. Neese, Dalton Trans. (2007) 1552.
[16] Unfortunately there is no single, all encompassing term to describe aminothiolate ligands. We have toyed with the idea of using "aminothiolenes" or "azathiolenes" but regrettably these are insufficient to embrace all the oxidation and protonation levels displayed by ligands of this type. Alas, we have retained the term "aminothiolate" throughout this manuscript irrespective of the state of the *N,S*-coordinated ligand. Perhaps due to a dearth of creativity, we have persisted with the regular abbreviations applied to the three redox levels; namely, abt = aminobenzenethiolate(1-), ibt = iminobenzenethiolate(2-), itbs = iminothiobenzosemiquinone(1-), with the different substitution pattern represented by the prefixed letters.
[17] A.L. Balch, F. Röhrscheid, R.H. Holm, J. Am. Chem. Soc. 87 (1965) 2301.
[18] (a) J.C. Noveron, R. Herradora, M.M. Olmstead, P.K. Mascharak, Inorg. Chim. Acta 285 (1999) 269;
(b) J.C. Noveron, M.M. Olmstead, P.K. Mascharak, Inorg. Chem. 37 (1998) 1138;
(c) N. Roy, S. Sproules, T. Weyhermüller, K. Wieghardt, Inorg. Chem. 48 (2009) 3783;
(d) D. Sellmann, J. Utz, F.W. Heinemann, Inorg. Chem. 38 (1999) 459.
[19] (a) B.K. Burgess, D.J. Lowe, Chem. Rev. 96 (1996) 2983;
(b) R.R. Eady, Chem. Rev. 96 (1996) 3013;
(c) J.B. Howard, D.C. Rees, Chem. Rev. 96 (1996) 2965;
(d) D.C. Rees, J.B. Howard, Curr. Opin. Chem. Biol. 4 (2000) 559.
[20] (a) I.G. Dance, J. Biol. Inorg. Chem. 1 (1996) 581;
(b) H. Deng, R. Hoffmann, Angew. Chem. Int. Ed. 32 (1993) 1062;
(c) M.D. Fryzuk, S.A. Johnson, Coord. Chem. Rev. 200–202 (2000) 379;
(d) D. Sellmann, A. Fürsattel, J. Sutter, Coord. Chem. Rev. 200–202 (2000) 545;
(e) D. Sellmann, J. Sutter, J. Biol. Inorg. Chem. 1 (1996) 587;
(f) K.K. Stravrev, M.C. Zerner, Chem. Eur. J. 2 (1996) 83.
[21] D. Sellmann, S. Emig, F.W. Heinemann, Angew. Chem. Int. Ed. 36 (1997) 1734.
[22] D. Sellmann, S. Emig, F.W. Heinemann, Angew. Chem. Int. Ed. 36 (1997) 1201.
[23] Originally this ligand was abbreviated with "bmae". In several subsequent publications, it is represented by 'N2S2'.
[24] According to current terminology, a *formal oxidation state* of a metal is determined by removing the ligand in their closed-shell form, whereas a *physical (or spectroscopic) oxidation state* is the d^n electron count established spectroscopically (Chaudhuri et al., J. Am. Chem. Soc. 123 (2001) 2213). A classic Werner-type coordination complex has the same *formal* and *physical* oxidation state, whereas the presence of radical ligands (open-shell) in a complex produces non-identical formal and *physical* oxidation states.
[25] P. Ghosh, A. Begum, E. Bill, T. Weyhermüller, K. Wieghardt, Inorg. Chem. 42 (2003) 3208.
[26] P. Ghosh, E. Bill, T. Weyhermüller, K. Wieghardt, J. Am. Chem. Soc. 125 (2003) 3967.
[27] A.K. Patra, E. Bill, T. Weyhermüller, K. Stobie, Z. Bell, M.D. Ward, J.A. McCleverty, K. Wieghardt, Inorg. Chem. 45 (2006) 6541.
[28] D. Coucouvanis, W. Swenson, N.C. Baenziger, C. Murphy, D.G. Holah, N. Sfarnas, A. Simopoulos, A. Kostikas, J. Am. Chem. Soc. 103 (1981) 3350.
[29] D. Coucouvanis, D.G. Holah, F.J. Hollander, Inorg. Chem. 11 (1975) 2657.
[30] K. Ray, A. Begum, T. Weyhermüller, S. Piligkos, J. van Slageren, F. Neese, K. Wieghardt, J. Am. Chem. Soc. 127 (2005) 4403.
[31] D. Sellmann, U. Kleine-Kleffmann, L. Zapf, G. Huttner, L. Zsolnai, J. Organomet. Chem. 263 (1984) 321.
[32] D. Sellmann, M. Geck, M. Moll, J. Am. Chem. Soc. 113 (1991) 5259.
[33] D. Sellmann, T. Becker, F. Knoch, Chem. Ber. 129 (1996) 509.
[34] V. Gama, R.T. Henriques, G. Bonfait, L.C. Pereira, J.C. Waerenborgh, I.C. Santos, M.T. Duarte, J.M.P. Cabral, M. Almeida, Inorg. Chem. 31 (1992) 2598.
[35] D. Simão, J.A. Ayllón, S. Rabaça, M.J. Figueira, I.C. Santos, R.T. Henriques, M. Almeida, Cryst. Eng. Commun. 8 (2006) 658.
[36] R. Yu, K. Arumugam, A. Manepalli, Y. Tran, R. Schmehl, H. Jacobsen, J.P. Donahue, Inorg. Chem. 46 (2007) 5131.
[37] (a) R. Eisenberg, Prog. Inorg. Chem. 12 (1970) 295;
(b) C.L. Beswick, J.M. Schulman, E.I. Stiefel, Prog. Inorg. Chem. 52 (2004) 55.
[38] (a) J.A. Ayllón, I.C. Santos, R.T. Henriques, M. Almeida, L. Alcacer, M.T. Duarte, Polyhedron 17 (1998) 4023;
(b) S. Boyde, C.D. Garner, J.H. Enemark, M.A. Bruck, J. Chem. Soc., Dalton Trans. (1987) 297;
(c) S. Boyde, C.D. Garner, J.H. Enemark, M.A. Bruck, J.G. Kristofzski, J. Chem. Soc., Dalton Trans. (1987) 2267;
(d) S. Lo Schiavo, F. Nicolo, R. Scopelliti, G. Tresoldi, P. Piraino, Inorg. Chim. Acta 304 (2000) 108;
(e) I.C. Santos, J.A. Ayllón, R.T. Henriques, M. Almeida, L. Alcacer, M.T. Duarte, Acta Crystallogr. C53 (1997) 1768;
(f) Y.-J. Zhao, W.-P. Su, R. Cao, M.-C. Hong, Acta Crystallogr. E57 (2001) m229.
[39] N. Roy, S. Sproules, E. Bill, T. Weyhermüller, K. Wieghardt, Inorg. Chem. 47 (2008) 10911.
[40] H. Jacobsen, J.P. Donahue, Inorg. Chem. 47 (2008) 10037.
[41] J.F. Weiher, L.R. Melby, R.E. Benson, J. Am. Chem. Soc. 86 (1964) 4329.
[42] A. Davison, N. Edelstein, R.H. Holm, A.H. Maki, Inorg. Chem. 3 (1964) 814.
[43] J.H. Enemark, W.N. Lipscomb, Inorg. Chem. 4 (1965) 1729.
[44] A.L. Balch, R.H. Holm, Chem. Commun. (1966) 552.
[45] G.N. Schrauzer, V.P. Mayweg, H.W. Finck, W. Heinrich, J. Am. Chem. Soc. 88 (1966) 4604.
[46] T. Yamaguchi, S. Masaoka, K. Sakai, Acta Crystallogr. E64 (2008) m1557.
[47] W.C. Hamilton, I. Bernal, Inorg. Chem. 6 (1967) 2003.
[48] B.S. Kang, L.H. Weng, D.X. Wu, F. Wang, Z. Guo, L.R. Huang, Z.Y. Huang, H.Q. Liu, Inorg. Chem. 27 (1988) 1128.
[49] D.T. Sawyer, G.S. Srivatsa, M.E. Bodini, W.P. Schaefer, R.M. Wing, J. Am. Chem. Soc. 108 (1986) 936.
[50] A.C. Cerdeira, D. Simão, I.C. Santos, A. Machado, L.C.J. Pereira, J.C. Waerenborgh, R.T. Henriques, M. Almeida, Inorg. Chim. Acta 361 (2008) 3836.
[51] H. Alves, D. Simão, H. Novais, I.C. Santos, C. Giménez-Saiz, V. Gama, J.C. Waerenborgh, R.T. Henriques, M. Almeida, Polyhedron 22 (2003) 2481.
[52] T. Yamaguchi, S. Masaoka, K. Sakai, Acta Crystallogr. E65 (2009) m77.
[53] J.V. Rodrigues, I.C. Santos, V. Gama, R.T. Henriques, J.C. Waerenborgh, M.T. Duarte, M. Almeida, J. Chem. Soc., Dalton Trans. (1994) 2655.
[54] X. Ren, P. Wu, W. Zhang, Q. Meng, X. Chen, Trans. Met. Chem. 27 (2002) 394.
[55] D. Bellamy, N.G. Connelly, G.R. Lewis, A.G. Orpen, Cryst. Eng. Commun. 4 (2002) 51.
[56] M. Fettouhi, L. Ouahab, M. Hagiwara, E. Codjovi, O. Kahn, H. Constant-Machado, F. Varret, Inorg. Chem. 34 (1995) 4152.
[57] M. Fettouhi, A. Waheed, S. Golhen, N. Helou, L. Ouahab, P. Molinié, Synth. Met. 102 (1999) 1764.
[58] S. Tanaka, G. Matsubayashi, J. Chem. Soc., Dalton Trans. (1992) 2837.
[59] K. Awaga, T. Okuno, Y. Maruyama, A. Kobayashi, H. Kobayashi, S. Schenk, A.E. Underhill, Inorg. Chem. 33 (1994) 5598.
[60] P. Deplano, L. Leoni, M.L. Mercuri, J.A. Schlueter, U. Geiser, H.H. Wang, A.M. Kini, J.L. Manson, C.J. Gómez-García, E. Coronado, H.-J. Koo, M.-H. Whangbo, J. Mater. Chem. 12 (2002) 3570.
[61] L. Pilia, C. Faulmann, I. Malfant, V. Collière, M.L. Mercuri, P. Deplano, P. Cassoux, Acta Crystallogr. C58 (2002) m240.
[62] M.G. Kanatzidis, D. Coucouvanis, Inorg. Chem. 23 (1984) 403.
[63] A. Schultz, R. Eisenberg, Inorg. Chem. 12 (1973) 518.
[64] S. Alvarez, R. Vicente, R. Hoffmann, J. Am. Chem. Soc. 107 (1985) 6253.
[65] (a) C. Mahadevan, M. Seshasayee, B.V.R. Murthy, P. Kuppusamy, P.T. Manoharan, Acta Crystallogr. C39 (1983) 1335;
(b) C. Mahadevan, M. Seshasayee, A. Radha, P.T. Manoharan, Acta Crystallogr. C40 (1984) 2032.
[66] R. Sarangi, S. DeBeer George, D. Jackson Rudd, R.K. Szilagyi, X. Ribas, C. Rovira, M. Almeida, K.O. Hodgson, B. Hedman, E.I. Solomon, J. Am. Chem. Soc. 129 (2007) 2316.
[67] I.G. Dance, Inorg. Chem. 12 (1973) 2748.
[68] D. Simão, H. Alves, D. Belo, S. Rabaça, E.B. Lopes, I.C. Santos, V. Gama, M.T. Duarte, R.T. Henriques, H. Novais, M. Almeida, Eur. J. Inorg. Chem. (2001) 3119.
[69] T. Birchall, N.N. Greenwood, J. Chem. Soc. A (1969) 286.
[70] T. Birchall, N.N. Greenwood, J.A. McCleverty, Nature 215 (1967) 625.
[71] J.A.W. Dalziel, J.D. Donaldson, B.D. Mehta, M.J. Tricker, J. Inorg. Nucl. Chem. 35 (1973) 3811.
[72] J.L.K.F. de Vries, J.M. Trooster, E. de Boer, Inorg. Chem. 10 (1971) 81.
[73] C. Faulmann, P. Cassoux, Prog. Inorg. Chem. 52 (2004) 399.
[74] S. Sproules, S.R. Presow, J. Witling, T. Weyhermüller, E. Bill, K. Wieghardt, in preparation.
[75] L.F. Larkworthy, J.M. Murphy, D.J. Phillips, Inorg. Chem. 7 (1968) 1436.
[76] D. Sellmann, O.Z. Käppler, Z. Naturforsch, B: Chem. Sci. 42b (1987) 1291.
[77] The published quadrupole splitting $\Delta E_Q = 0.93\ mm\ s^{-1}$ is erroneous; the true value is $\Delta E_Q = 2.83\ mm\ s^{-1}$ which is consistent with an intermediate-spin Fe(III) ion.
[78] (a) P. Ghosh, A. Begum, D. Herebian, E. Bothe, K. Hildenbrand, T. Weyhermüller, K. Wieghardt, Angew. Chem. Int. Ed. 42 (2003) 563;
(b) D. Herebian, E. Bothe, E. Bill, T. Weyhermüller, K. Wieghardt, J. Am. Chem. Soc. 123 (2001) 10012.
[79] D. Sellmann, O.Z. Käppler, F. Knoch, M. Moll, Z. Naturforsch, B: Chem. Sci. 45b (1990) 803.
[80] Glyoxal-bis-(2-mercaptoanil), H2gma, is a well-studied tetradenate bis(aminothiolate) ligand that is bridged with an unsaturated ethylene unit. It forms dinuclear complexes with iron that are readily cleaved by Lewis bases. Although its connectivity is similar to other tetradentate aminothiolate ligands, it is unique in that the α-diimine linkage that is the redox active compontent (Ghosh et al., J. Am. Chem. Soc. 125 (2003) 1293, and references therein). As such, it is not included in this review.
[81] D. Sellmann, U. Reineke, J. Organomet. Chem. 314 (1986) 91.
[82] R. Williams, E. Billig, J.H. Waters, H.B. Gray, J. Am. Chem. Soc. 88 (1966) 43.
[83] N.G. Connelly, J.A. McCleverty, C.J. Winscom, Nature 216 (1967) 999.
[84] J.A. McCleverty, N.M. Atherton, N.G. Connelly, C.J. Winscom, J. Chem. Soc. A (1969) 2242.
[85] J.K. Yandell, N. Sutin, Inorg. Chem. 11 (1972) 448.
[86] I.G. Dance, T.R. Miller, Inorg. Chem. 13 (1974) 525.
[87] G.R. Eaton, R.H. Holm, Inorg. Chem. 10 (1971) 805.
[88] S. Friedle, D.V. Partyka, M.V. Bennett, R.H. Holm, Inorg. Chim. Acta 359 (2006) 1427.
[89] M. Fettouhi, M. Morsy, A. Waheed, S. Golhen, L. Ouahab, J.-P. Sutter, O. Kahn, N. Menendez, F. Varret, Inorg. Chem. 38 (1999) 4910.

[90] J.-P. Sutter, M. Fettouhi, L. Li, C. Michaut, L. Ouahab, O. Kahn, Angew. Chem. Int. Ed. 35 (1996) 2113.
[91] A.K. Patra, E. Bill, E. Bothe, K. Chłopek, F. Neese, T. Weyhermüller, K. Stobie, M.D. Ward, J.A. McCleverty, K. Wieghardt, Inorg. Chem. 45 (2006) 7877.
[92] E.F. Epstein, I. Bernal, Chem. Commun. (1970) 136.
[93] (a) D. Sellmann, N. Blum, F.W. Heinemann, Z. Naturforsch, B: Chem. Sci. 56 (2001) 581;
(b) D. Sellmann, N. Blum, F.W. Heinemann, B.A. Hess, Chem. Eur. J. 7 (2001) 1874;
(c) D. Sellmann, K.P. Peters, F.W. Heinemann, Eur. J. Inorg. Chem. (2004) 581;
(d) D. Sellmann, S.Y. Shaban, F.W. Heinemann, Eur. J. Inorg. Chem. (2004) 4591;
(e) D. Sellmann, J. Sutter, Prog. Inorg. Chem. 52 (2004) 585.
[94] K. Chłopek, N. Muresan, F. Neese, K. Wieghardt, Chem. Eur. J. 13 (2007) 8390.
[95] A.L. Balch, Inorg. Chem. 6 (1967) 2158.
[96] J.A. McCleverty, D.G. Orchard, J. Chem. Soc. A (1971) 626.
[97] J.A. McCleverty, B. Ratcliff, J. Chem. Soc. A (1970) 1631.
[98] A.A. Vlcek, Prog. Inorg. Chem. 5 (1963) 211.
[99] E.F. Epstein, I. Bernal, Inorg. Chim. Acta 25 (1977) 145.
[100] H. Miyamae, S. Sato, Y. Saito, K. Sakai, M. Fukuyama, Acta Crystallogr. B33 (1977) 3942.
[101] D. Sellmann, S. Emig, F.W. Heinemann, F. Knoch, Z. Naturforsch, B: Chem. Sci. 53 (1998) 1461.
[102] (a) H. Chun, T. Weyhermüller, E. Bill, K. Wieghardt, Angew. Chem. Int. Ed. 40 (2001) 2489;
(b) H. Chun, E. Bill, T. Weyhermüller, K. Wieghardt, Inorg. Chem. 42 (2003) 5612.
[103] C.C. McDonald, W.D. Phillips, H.F. Mower, J. Am. Chem. Soc. 87 (1965) 3319.
[104] J.A. McCleverty, B. Ratcliff, J. Chem. Soc. A (1970) 1627.
[105] A.I.M. Rae, Chem. Commun. (1967) 1245.
[106] J. Locke, J.A. McCleverty, E.J. Wharton, C.J. Winscom, Chem. Commun. (1967) 1289.
[107] P. Ghosh, K. Stobie, E. Bill, E. Bothe, T. Weyhermüller, M.D. Ward, J.A. McCleverty, K. Wieghardt, Inorg. Chem. 46 (2007) 522.
[108] P. Ghosh, E. Bill, T. Weyhermüller, K. Wieghardt, Inorg. Chem. 46 (2007) 2612.
[109] J.H. Enemark, R.D. Feltham, Coord. Chem. Rev. 13 (1974) 339.
[110] C.-M. Lee, C.-H. Chen, H.-W. Chen, J.-L. Hsu, G.-H. Lee, W.-F. Liaw, Inorg. Chem. 44 (2005) 6670.
[111] G. Teschmit, R. Kirmse, Inorg. Chem. Commun. 2 (1999) 465.
[112] S. Chatel, A.-S. Chauvin, J.-P. Tuchagues, P. Leduc, E. Bill, J.-C. Chottard, D. Mansuy, I. Artaud, Inorg. Chim. Acta 356 (2002) 19.
[113] C.-M. Lee, C.-H. Hsieh, A. Dutta, G.-H. Lee, W.-F. Liaw, J. Am. Chem. Soc. 125 (2003) 11492.
[114] M. Li, D. Bonnet, E. Bill, F. Neese, T. Weyhermüller, N. Blum, D. Sellmann, K. Wieghardt, Inorg. Chem. 41 (2002) 3444.
[115] J.A. McCleverty, D.G. Orchard, K. Smith, J. Chem. Soc. A (1971) 707.
[116] C. Milsmann, S. Sproules, E. Bill, T. Weyhermüller, S. DeBeer George, K. Wieghardt, Chem. Eur. J. 16 (2010) accepted.
[117] J.A. McCleverty, J. Locke, E.J. Wharton, M. Gerloch, J. Chem. Soc. A (1968) 816.
[118] J.A. McCleverty, E.J. Wharton, J. Chem. Soc. A (1969) 2258.
[119] R. Rickards, C.E. Johnson, H.A.O. Hill, J. Chem. Soc. A (1971) 797.
[120] R.L. Carlin, F. Canziani, J. Chem. Phys. 40 (1964) 371.
[121] (a) S.A. Cotton, J.F. Gibson, Chem. Commun. (1968) 883;
(b) S.A. Cotton, J.F. Gibson, J. Chem. Soc. A (1971) 803.
[122] L.H. Pignolet, G.S. Patterson, J.F. Weiher, R.H. Holm, Inorg. Chem. 13 (1974) 1263.
[123] (a) G.R. Lewis, I. Dance, J. Chem. Soc., Dalton Trans. (2000) 3176;
(b) A. Sequeira, I. Bernal, J. Cryst. Mol. Struct. 3 (1973) 157.
[124] K. Chłopek, E. Bill, T. Weyhermüller, K. Wieghardt, Inorg. Chem. 44 (2005) 7087.